STUDY OF STRUCTURAL AND ELECTRONIC PROPERTIES OF ALKALINE EARTH METAL CALCIUM AND STRONTIUM

A Dissertation

Submitted for the Partial Fulfillment of

Requirements for the Masters of Science Degree in Physics

Shiva Prasad Bhusal

T.U. Registration No: 5-2-19-709-2008

Symbol No: Phy. 1316/072

DEPARTMENT OF PHYSICS

INSTITUTE OF SCIENCE AND TECHNOLOGY

BIRENDRA MULTIPLE CAMPUS,

BHARATPUR CHITWAN

October, 2020

©Tribhuvan University

DECLARATION

I, "Shiva Prasad Bhusal", hereby declare that the work presented here is genuine work done originally by me and has not been published or submitted elsewhere for the requirement of a degree program. Any literature, data or works done by others and cited in this dissertation has been given due acknowledgement and listed in the reference.

_____

Shiva Prasad Bhusal

Date:

RECOMMENDATION LETTER

This is to certify that the dissertation work entitled **STUDY OF STRUCTURAL AND ELECTRONIC PROPERTIES OF ALKALINE EARTH METAL CALCIUM AND STRONTIUM** has been carried out by **Mr. Shiva Prasad Bhusal** as the partial fulfillment for the requirement of M.Sc. Degree in Physics under our supervision. To the best of my knowledge, this work is original and is not been submitted to any other degree in this institute.

…….

Supervisor

Prof. Dr. Sitaram Bahadur Thapa

Department of Physics

Birendra Multiple Campus

Tribhuvan University

Bharatpur, Nepal

Date…….

…….

Supervisor

Dr. Rajendra Prasad Adhikari

Department of Natural Science (Applied Physics)

Kathmandu University

Dhulikhel, Kavre

Date…….

EVALUATION

ABSTRACT

We optimize lattice parameter and identify the nature and values of band gap of Calcium and Strontium using quantum espresso. This piece includes the general introduction on crystal structure and different models that work in the lattice constant and lattice dynamic. We also attempt to briefly include various Theoretical details such as Born-Oppenheimer Approximation, Hartree-Fock Approximation, Density Functional Theory, Kohn-Sham approach, Local Density approximation, Generalized Gradient Approximation, and pseudo- potential. Finally, we discussed the fundamentals of Quantum Espresso computational program with the result and discussion on electronic properties, kinetic energy cut-off, lattice parameter, band gap, density of state and partial density of state.

During optimization, the kinetic energy cut-off energy is found to be 90 Ry having k-point grid $6 \times 6 \times 6$ for Ca. Then we estimate the lattice Parameter is found to be 10.46 Bohr for Ca which is very near with experimental results as well as previous calculated data. Which is only 0.95% deviated from experimental result and previous data. Thus the lattice parameter of Ca estimated with GGA method is in close agreement with experimental values. Then we have study the band structure, density of states and partial density of states of Ca using GGA method in QE package.

Similarly, optimization, the kinetic energy cut-off energy is found to be 110 Ry having k-point grid $4 \times 4 \times 4$ for Sr. Then we estimate the lattice Parameter is found to be 11.49 Bohr for Sr which is very near with experimental results as well as previous calculated data. Which is only 0.9% deviated from experimental result and previous data. Thus the lattice parameter of Sr estimated with GGA method is in close agreement with experimental values. Then we have study the band structure, density of states and partial density of states of Ca using GGA method in QE package.

ACKNOWLEDGEMENTS

During the study and completion of this Dissertation I have benefited from many peoples to whom I would like to express my sincere thanks.

In this insightful delight I would first of all convey my sincere gratefulness to my supervisors **Prof. Dr. Sitaram Bahadur Thapa** and **Dr. Rajendra P. Adhikari** for providing me intellectual suggestions and very useful guidance without whose companionship of my thesis would ever have come to this stage.

Also, I am equally thankful to The **former campus chief Mr. Govinda Sapkota, campus chief Prof. Dayaram Poudel, Head of the Department Prof. Arun Kumar Shrestha.** I also express my sincere thanks to Prof. Dr. Harihar poudyal, Associate Prof. Dilli Prasad Sapkota, Dr. Seshkant Adhikari, Mr. Ekraj Poudel, Mr. Rajendra Neupane, Mr. Uday Bahadur Thapa, Mr. Ram Krishna Tiwari, Mr. Sanjay Shah, Mr. Rabindra Raj Bista, Mr. Madan Phuyal, Mr. Moti Bhusal, Mr. Ishwor Chandra Poudel, Mr. Pratap Koirala Mr. Rudra Poudel and all the respected faculty members of Physics Department of Birendra Multiple Campus.

The acknowledgement would be incomplete if I don't mention my friends Mr. Dhruba Sapkota, Mr. Amrit Sharma, Mr. Shiva Prasad Bhusal and Mr. Surya Prasad Ghimire for their consistent help and warm support during this work.

I would like to remember my family, their support and encouragement. This work would not have been possible without the love and patience of my family. So, I want to give huge respect to my father Mr. Pareswar Bhusal, mother Mrs. Manrupa Bhusal, and my brothers Ujwal, Manoj and Utsav. I am also thankful to all my friends , relatives and well wishers for their valuable support and suggestions during this project.

It is impossible to remember all to whom I owe my gratitude, and I apologize to those I've inadvertently left out.

Shiva Prasad Bhusal
Birendra Multiple Campus
Bharatpur-10, Chitwan

TABLE OF CONTENTS

LIST OF TABLES

LIST OF FIGURES

LIST OF ABBREVIATIONS

BO	:	Born Oppenheimer
CP	:	Car-Perrinello
CPMD	:	Car-Parrinello Molecular Dynamics
DFPT	:	Density Functional Perturbation Theory
DFT	:	Density Functional Theory
DOS	:	Density of State
FPMD	:	First Principle Molecular Dynamics
GGA	:	Generalized Gradient Approximation
HEG	:	Homogeneous Electron Gas
HF	:	Hartree-Fock
HK	:	Hohenberg-Kohn
KS	:	Kohn-Sham
LDA	:	Local Density Approximation
MBE	:	Molecular Beam Epitaxy
MOVPE	:	Metalorganic Vapour Phase Epitaxy
NSCF	:	Non-Self Consistent Field
PBE	:	Perdew, Burke and Ernzerhof
PDOS	:	Partial Density of State
PP	:	Pseudo Potential
PW	:	Plane Wave
QE	:	Quantum ESPRESSO
SCF	:	Self Consistent Field
XC	:	exchange Correlation

CHAPTER 1

INTRODUCTION

1.1 General Consideration

The solidification or freezing of matter may lead to formation of ordered or disordered state in which ordered state is known as crystalline state where as the disordered one is termed the amorphous state. Crystalline state refers to an infinitive array of atoms or a group of atoms. The whole volume of crystal is constructed by moving block of smallest size along its edges which block is called a unit cell. The three-dimensional structure of a crystal is built from a repetitive arrangement of the simplest structural unit, called the unit cell, just as a single tile is often a unit cell for a two-dimensional ceramic tiling pattern. It received direct experimental configuration in 1913 through the work of W. and L. Bragg, who founded the subject of X-ray crystallography and began investigation of ow atoms arranged in solids. Depending on the nature of the unit cell, Bragg's law is satisfied only at certain orientations of the crystal, and a beam of X-rays will then emerge from the crystal at a certain angle to the incident beam. Bragg's law requires that the diffracted radiation from different layers of unit cells be in phase [1]. Every crystal structure satisfies the requirements of a specific group of certain *symmetry operation* (to show visualization of motional operations performed on atoms with unit cell). Different combination of symmetry operations results in different crystal structure.

crystal

Crystals may be classified in terms of the dominant type of chemical binding force keeping the atoms together. All these bonds involve electrostatic forces, with the chief differences among them lying in the ways in which the outer electrons of the structural elements are distributed. The distinct types of bonds that provide the cohesive forces in crystals can be classified as follows: (i)

the ionic bond (ii) the covalent bond (iii) the metallic bond (iv) the van der Waals bond and (v) the hydrogen bond. We briefly discuss the different types of bonds in crystals.

The ionic bond

The electron state is little affected by the coming together of the ions to from the solid and the interaction of any two ions within the solid can be represented by the inter ionic potential curve of two isolated ions. At large separation the inter ionic potential is dominated by the long-range electrostatic interaction $\frac{\pm e^2}{4\pi\varepsilon_0 r;}$ the +sign for two ions of same sign and -sign for ions of opposite sign [2].

The covalent bond

In the covalent bonded crystal, the binding energy is associated with the sharing of valence electrons between atoms. The states of the valence electrons are profoundly changed by the approach of the atoms to form the solid, and where an atom forms more than one bond the energy depends strongly on their relative orientation. A pair of electrons is necessary feature of covalent bond, an atom cannot in general form more bonds than valence electrons. In an ideal covalent bond between two atoms the two electrons are equally shared.

The metallic bonding

Metallic bonding, which is formed when electrons are shared by all the atoms in the solid, producing a uniform "sea" of negative charge; the solids produced in this way are the usual metals.

The Vander Wall Bond

It is an additional type of bond. However, the vander Waals bond is only significant in case where other types of bonding are not possible, for example, between atoms with closed electron shell, or between saturated molecules. The physical source of this bonding is charge fluctuations in the atoms due to zero-point motion. Vander Waal forces are responsible for the bonding in molecular crystals. The bonding energy is dependent on the polarizability of the atoms involved

and is mostly of order of 0.1eV. Typical atomic bonding radii for van der Waals bonding are considerably larger than for chemical bonding

The Hydrogen Bond

In a chemical bond when a atom is bond to 2 other atoms. At first, it's surprising that such a bond can exist since hydrogen has just one electron. However, one can imagine the chemical bond as follows: when hydrogen takes part during a chemical bond with a strongly electronegative atom, for instance, oxygen, its single electron is nearly completely transferred to partner atom. The proton which remain can then exert a beautiful force on a second negative atom and very small size of the proton with its strongly reduced electron screening, it's impossible for a 3rd atom to be bound. Generally, speaking, the phenomena related to hydrogen bonding are quite diverse and this sort of bonding is harder to characterize than most other types. The binding energies of hydrogen bonds are of the order of 0.1eV per bond [3].

An infinite array of points in space called a lattice (space lattice) and arrangement of points defined the lattice symmetry. when an atom or a uniform group of atom s attached to each lattice point, we get a crystal structure. The attached atom or group of atoms called basis, which is identical for each lattice point in terms of composition, relative orientation, and separation. The lattice is defined by three fundamental translation vector a, b and c such the atomic arrangement looks an equivalent in every respect when viewing from the purpose r as when viewed from the purpose . Draw a vector t connecting two lattice point P1 and P2 (fig 1.1) represent vectors r1 and r2 respectively then, the vector t is defined as

$$r_2 = r_1 + t$$

Such that

$$t = n_1 a + n_2 b + n_3 c$$

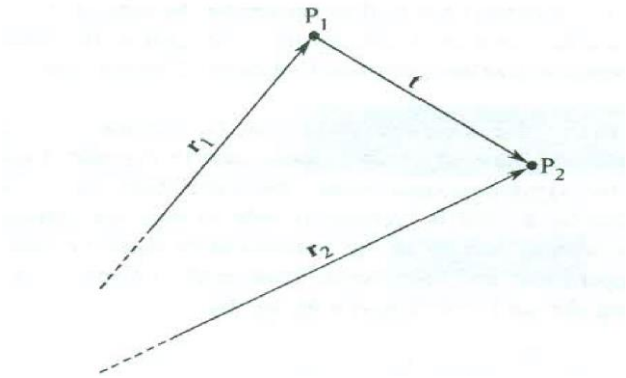

Fig. 1.1: Two lattice points P_1 and P_2 of a three-dimensional lattice connected by translation vector t[4]**.**

When all the lattice points can be located for the arbitrary choice of only integral values of n_1, n_2 and n_3, the crystal axes **a, b** and **c** are called primitive and the resulting unit is called *primitive cell.* A lattice is a mathematical abstraction; the crystal structure is formed when a basis of atom is attached identically to every lattice point. The logical relation is

Lattice + basis = crystal structure

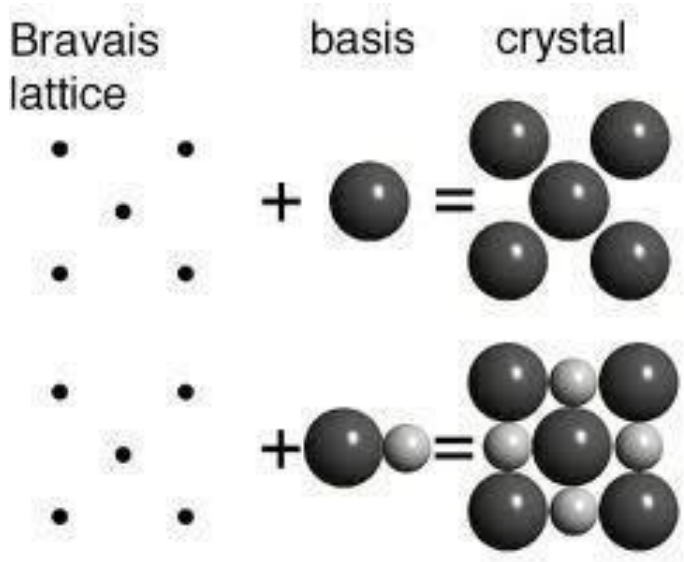

Fig 1.2: crystal structure[5]

An alternate primitive cell is known as Wigner-Seitz cell. A lattice point is joined to all the nearby lattice point s with the help of lattice vectors. Then, a plane perpendicular to each of these vectors, connecting the central lattice point, is draw at the midpoint of the vector. The planes

form a completely closed polyhedron which contains one lattice point at the centre which is named Wigner and Seitz [6]. Figure 1.3 shows the pictures of cell in two-dimension lattice.

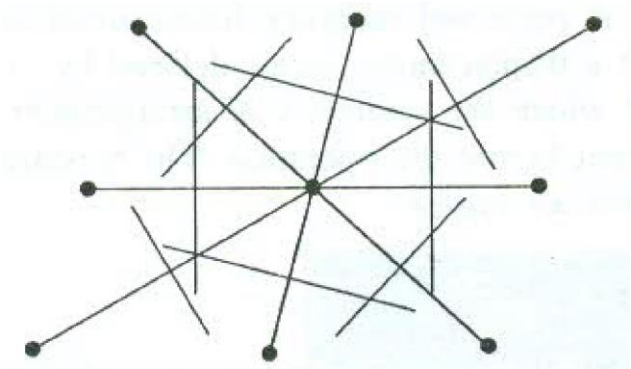

Fig.1.3: The construction of Wigner-Seitz cell for a two-dimensional space lattice[7].

Lattice planes and miller indices

A well-formed crystal or internal planes through a crystal structure are laid out in terms of Miller Indices, h, k, and l, written in round brackets, (hkl). an equivalent terminology is employed to specify planes during a lattice. Miller indices, (hkl), represent not only one plane, but the set of all identical parallel lattice planes. The values of h, k and l are the reciprocals of the fractions of a unit edge, a, b and c respectively, intersected by an appropriate plane. this suggests that a group of planes that lie parallel to a unit edge is given the index 0 (zero) no matter the lattice geometry. Thus, a group of planes that transit the ends of the unit cells, cutting the a-axis at an edge 1 a, and parallel to the b- and c-axes of the unit has Miller indices (100), (Figure 1.4a, b). an equivalent principles apply to the opposite planes shown. The set of planes that lies parallel to the a- and c-axes, and intersecting the top of every unit at an edge 1 b have Miller indices (010), (Figure 1.4c, d). The set of planes that lies parallel to the a- and b-axes, and intersecting the top of every unit at an edge 1 c have Miller indices (001), (Figure 1.4e, f). Planes cutting both the a-axis and b-axis at 1 a and 1 b are going to be (110) planes, (Figure 1.4 g,h), and planes cutting the a-, b- and c-axes at 1 a, 1 b and 1 c are going to be (111).

Remember that the Miller indices ask a family of planes, not only one . for instance , Figure 1.5 shows a part of the set of (122) planes, which cut the unit edges at 1 a, ½ b and ½ c. The Miller indices for lattice planes are often determined employing a simple method [5].

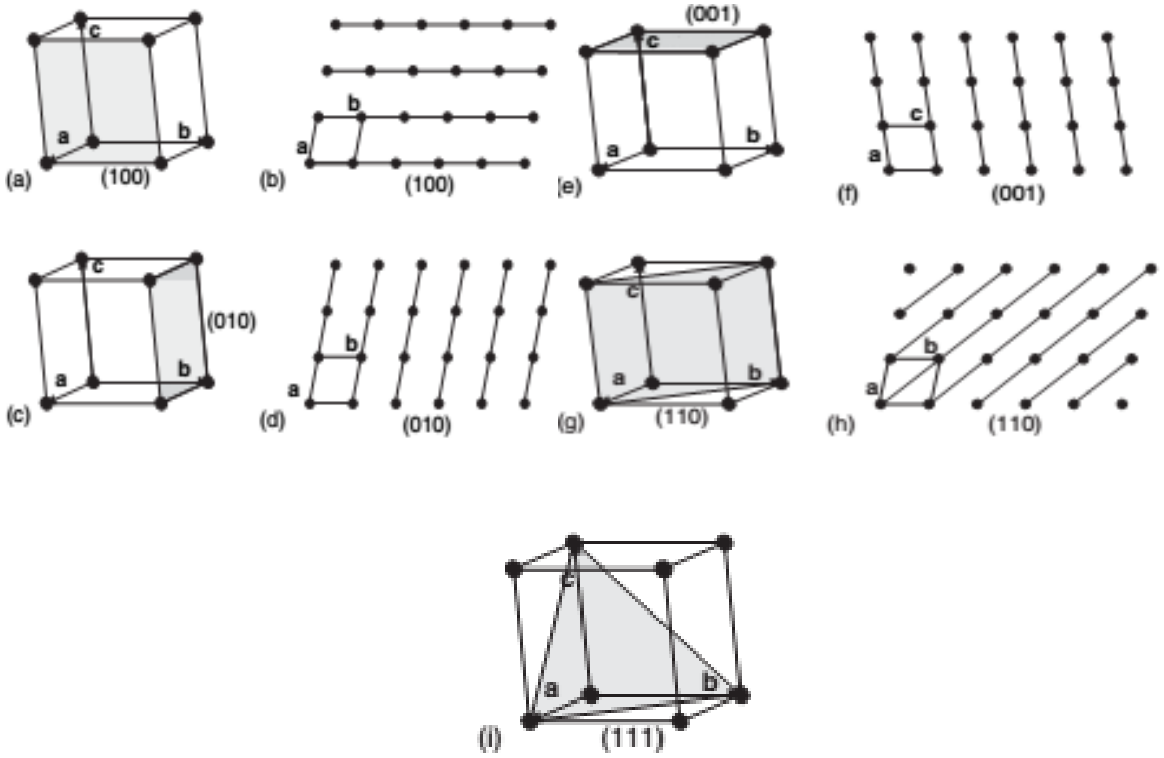

Figure 1.4 Miller indices of lattice planes: (a, b) (100); (c, d) (010); (e, f) (001), (g, h) (110); (i) (111)[8]

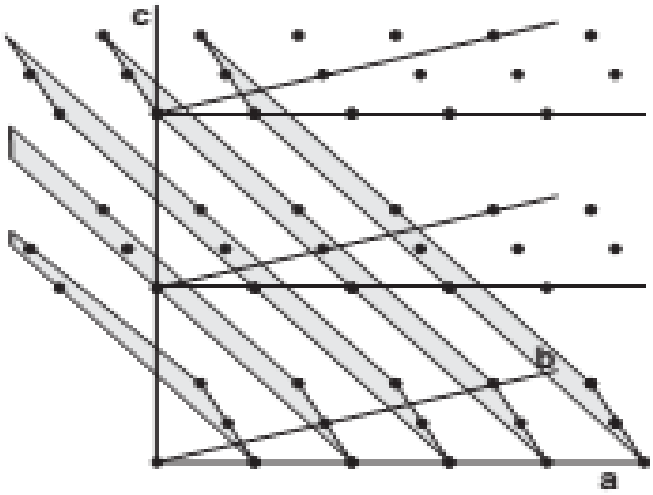

Figure 1.5: Part of the set of (122) lattice planes Bravais lattice in two dimensions[9]

The five Bravais lattice that can be received in two-dimension are depicted in fig.1.6*a* along with the primitive cell

Here they are described in terms of the elementary translation vectors $\mathbf{a}_1$ and $\mathbf{a}_2$ and of the angle ϕ that they form:

Properties

P1. Squared: $|\mathbf{a}_1| = |\mathbf{a}_2|$ and $\mathbf{a_1}$, $\mathbf{a_2}$ placed at angle $\varphi = \pi/2$

P2. Rectangular: $|\mathbf{a}_1| \neq |\mathbf{a}_2|$, and $\phi = \pi/2$

P3. Body-centered rectangular: As in the rectangular case in P2, but an extra lattice point is located at the canter of each rectangle. Note that this is a cell with two lattice points, located at centre and vertex positions of the rectangle. A cell including more than one lattice site and designed to have all the symmetries of the given lattice is usually named convention a cell. In particular, here the conventional cell is actually not the primitive cell. The latter can instead be represented considering the cell origin at the rectangle center and choosing a1 and a2 to be the vectors connecting the center with two vertexes of the same rectangle. In this representation, $|\mathbf{a}_1| = |\mathbf{a}_2|$ but $\phi \neq \pi/2$.

P4. Slanted or oblique: $|\mathbf{a}_1| \neq |\mathbf{a}_2|$and $\phi \neq \pi/2$.

P5. Hexagonal: $|\mathbf{a}_1| = |\mathbf{a}_2|$and $\phi = 2\pi/3$.

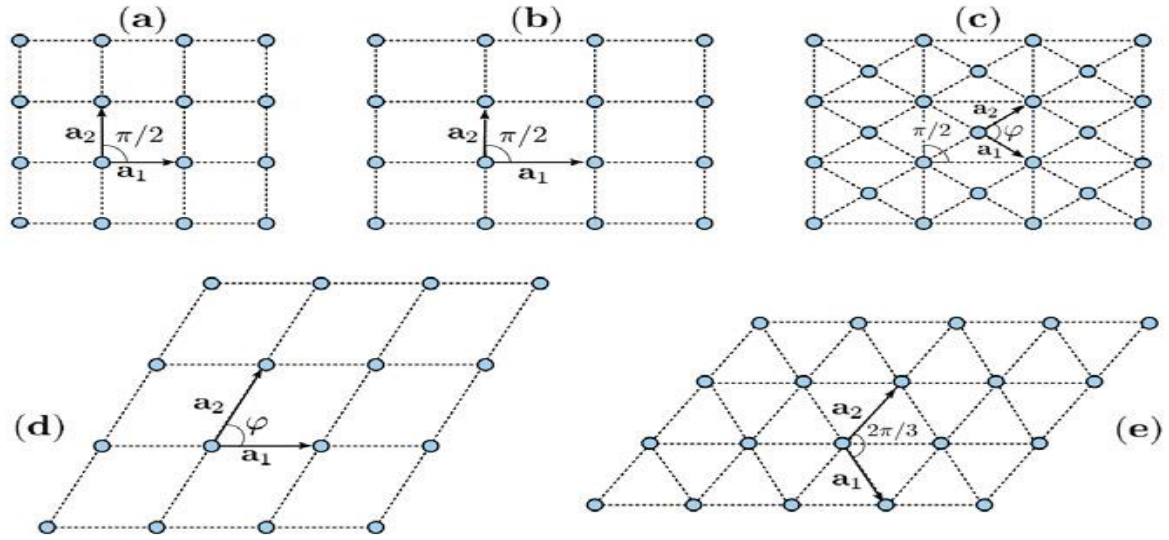

Fig. 1.6: Bravais lattice in 2D. The five conceivable Bravais lattices in 2D are depicted from (a) to (e)

The point-group symmetries related to these 5 lattices are easily picked out. Starting from that with lower symmetry, the slanted lattice in P4 has binary-axes symmetries. To the above binary-axes symmetries, the rectangular P2 and the body-centered rectangular P3 add reflections with respect to the straight-dashed lines in Fig. 1.4 (b) or any other straight line parallel to the latter and crossing at the rectangles centers. The squared lattice in P1 adds qua-ternary axes symmetries. Finally, the hexagonal P5 has ternary and scenery-axes symmetries, besides reflection symmetries. Note the peculiarity here that two different Bravais lattices, the rectangular and the body-centered rectangular, share the same point-group symmetry.

Three-Dimension Lattice Types

The point symmetry group in thee dimension require the 14 different lattice types listed in Table 1. The general lattice is triclinic, and there are 13 special lattices. These are grouped for convenience into systems classified according to seven types of cells, which are triclinic, monoclinic, orthorhombic, tetragonal, cubic, trigonal, and hexagonal. The division into systems

is expressed in the table in terms of the axial relations that describe the cells. The cells in Fig. 6 are conventional cells: of these only the (SC) is a primitive cell. Often a nonprimitive cell has a more obvious relation with the point symmetry operations than has a primitive cell. There are three lattices in the cubic system: the simple cubic (SC) lattice, the body-centered cubic (HCC) lattice, and the face-centered cubic (FCC) lattice

Cubic System

The point-group symmetries are those which leave a cube unchanged and can be counted in the number of 48. Three different Bravais lattices are classified in the cubic system: simple cubic, body-centered cubic and face-centered cubic. All of them are described below, since a great variety of materials occur in either one of these structures.

Tetragonal system

A tetragonal lattice is originated by a cube that is transformed into a parallelepiped with square base. Two different Bravais lattices are classified in the tetragonal system: simple and body-centered tetragonal lattice.

Orthorhombic system

The orthorhombic system is originated from the tetragonal one, after relaxing the requirement that the base be squared. Four different Bravais lattices are classified in the orthorhombic system: simple, base-centered, body-centered, and face-centered orthorhombic lattice.

Monoclinic system

The monoclinic system is originated from the orthorhombic ones, after making the base to be a rhomb. Two different Bravais lattices are classified in the monoclinic system, simple and face-centered.

Triclinic system

The triclinic system is originated from the monoclinic one, after slanting vector $\mathbf{a}_3$ with respect to the direction orthogonal to the plane containing $\mathbf{a}_1$ and $\mathbf{a}_2$.

Trigonal system

The trigonal system is originated from the simple cubic lattice, after deforming the cube along its diagonal: all the faces are rhombus, and each vertex is composed of three corners, each two of them forming the same angle.

Hexagonal system

The hexagonal system is obtained by layering hexagonal lattice planes one on top of the other, at distance *c*. The layering is arranged so that corresponding lattice points in adjacent planes are connected by lines perpendicular to the planes [10].

Table 1.1: Different types of lattice system [11]

System	Bravais lattice	unit cell characteristics	Characteristics symmetry elements
Cubic	Simple Body centered Face centered	a = b = c $\alpha = \beta = \gamma = 90°$	Four 3-fold rotation axes (along cube diagonal)
Tetragonal	Simple Body centered	a = b ≠ c $\alpha = \beta = \gamma = 90°$	One fourfold rotation axis
Orthorhombic	Simple Base centered Body centered Face centered	a≠ b ≠ c $\alpha = \beta = \gamma = 90°$	Three mutually orthogonal 2-fold rotation axes.
Monoclinic	Simple Base centered	a≠ b ≠ c $\alpha = \beta = 90° \neq \gamma$	One twofold rotation axis
Triclinic	Simple	a≠ b ≠ c $\alpha \neq \beta \neq 90° \neq \gamma$	None
Trigonal(rhombohedra)	Simple	a = b = c $\alpha = \beta = \gamma \neq 90$	One threefold rotation axis
Hexagonal	Simple	a = b = c $\alpha = \beta = 90$ $\gamma = 120$	One threefold rotation axis

The unit cell of a crystal is defined as that volume of space that its translations allow all the space without intervals and superpositions to be covered. The PUC is the minimal volume V**a** = a1[a2 × a3] unit cell connected with one Bravais lattice point. Conventional unit cells are defined by two, four and two lattice points, for the base-, face- and body-centered lattices, respectively.\

Table 1.2: Characteristics of cubic lattices[12]

Simple	body-centered	Face-centered
Volume, conventional call	a^3	a^3	a^3
Lattice Points per cell	1	2	4
Volume primitive cell	a^3	$\frac{1}{2}a^3$	$\frac{1}{4}a^3$
Lattice points per unit volume	$\frac{1}{a^3}$	$\frac{2}{a^3}$	$\frac{4}{a^3}$
Number of nearest neighbours	6	8	12
Nearest-neighbour distance	a	$3^{\frac{1}{2}}\frac{a}{2} = 0.866a$	$\frac{a}{2^{\frac{1}{2}}} = 0.707a$
Number of second neighbours	12	6	6
Second neighbour distance	$2^{\frac{1}{2}}a$	a	a
Packing Fraction	$\frac{1}{6}\pi$=0.524	$\frac{1}{6}\pi\sqrt{3}$=0.680	$\frac{1}{6}\pi\sqrt{3}$=0.740

Miller indices

All the faces of crystal can be described and numbered in terms of their axial intercepts where, axes represent crystallographic axes which are chosen to fit the symmetry; one or more of these axes may be axes of symmetry or parallel to them, but three convenient crystal edges be used if desire. The intercept *X*, *Y* and *Z* of this plane on the axes *x, y* and *z* are called parameters ***a, b*** and ***c***. the ratio of parameter ***a: b*** and ***b:c*** are called the axial ratios, and by convention the values of parameters are reduced so that value of b is unity. W. H. Miller suggested in 1839, that each face of crystal could be represented by the indices *h*, *k* and *l*, defined by [8]

$$h = \frac{a}{X}, k = \frac{b}{Y}, l = \frac{c}{Z}$$

The Reciprocal Lattice

The set of all wave vectors K that yield plane waves with the periodicity of a given Bravais lattice is known as its reciprocal lattice. Analytically, K belongs to reciprocal lattice of Bravais lattice of point R. so we characterize the reciprocal lattice as the set of wave vectors K satisfying

$$e^{i\vec{K}.\vec{R}} = 1$$

For all R in Bravais lattice

That the reciprocal lattice is itself a Bravais lattice follow most simply from the definition of Bravais lattice. Let $\mathbf{a_1}$, $\mathbf{a_2}$, and $\mathbf{a_3}$ be a set of primitive vectors for the direct lattice. Then reciprocal lattice can be generated by three Primitive vectors

$$\overrightarrow{b_1} = 2\pi \frac{\overrightarrow{a_2} \times \overrightarrow{a_3}}{\overrightarrow{a_1}(\overrightarrow{a_2} \times \overrightarrow{a_3})}$$

$$\overrightarrow{b_2} = 2\pi \frac{\overrightarrow{a_3} \times \overrightarrow{a_1}}{\overrightarrow{a_1}(\overrightarrow{a_2} \times \overrightarrow{a_3})}$$

$$\overrightarrow{b_3} = 2\pi \frac{\overrightarrow{a_1} \times \overrightarrow{a_2}}{\overrightarrow{a_1}(\overrightarrow{a_2} \times \overrightarrow{a_3})}$$

For all K in reciprocal lattice,where $K = k_1 b_1 + k_2 b_2 + k_3 b_3$ [9]

The Brillouin zone construction gives the all wave vectors which suffer diffraction from the crystal [12]. The first Brillouin zone has the shape of the truncated octahedron.

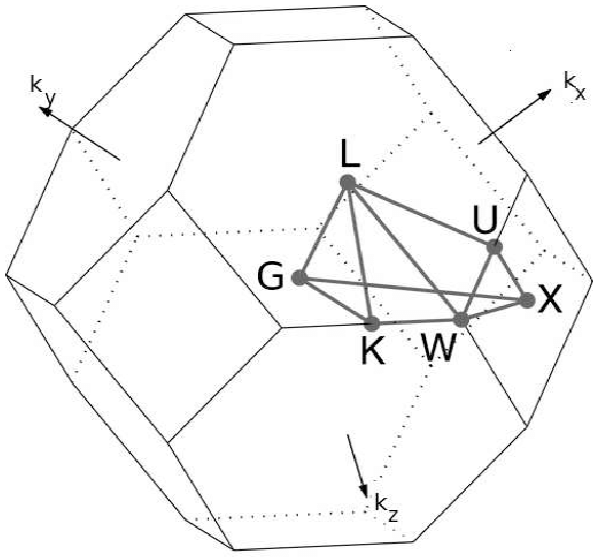

Figure 1.7: Brillouin zone[13]

Density of states

We may find the number of energy levels $dN(E)$ within energy interval E and $E + dE$ (or with *n* between *n* and *n + dn)* by counting the number of points that lie in a spherical shell or radius *E* and thickness *dE*. It may be noted here that although the energy *E* (and therefore *n*) is quantized, the spacing between the successive energy levels becomes infinitesimally small as *L* becomes large. We can then treat E and therefore n as continuous variables. Then energy interval dE corresponds to an interval dn given by

$$dE = \frac{\hbar^2\pi^2}{2mL^2} \times 2ndn,$$

Now the number of points in the positive octant of a spherical shell of radius n and thickness dn is $dN = \frac{1}{8} \times 4\pi n^2 dn$. we find

$$dN(E) = \frac{1}{4\pi^2}\left[\frac{2m}{\hbar^2}\right]^{\frac{3}{2}} L^3\sqrt{E}dE = \frac{1}{4\pi^2}\left[\frac{2m}{\hbar^2}\right]^{\frac{3}{2}} V\sqrt{E}dE$$

Where, V is the volume of the box (occupied by the system).

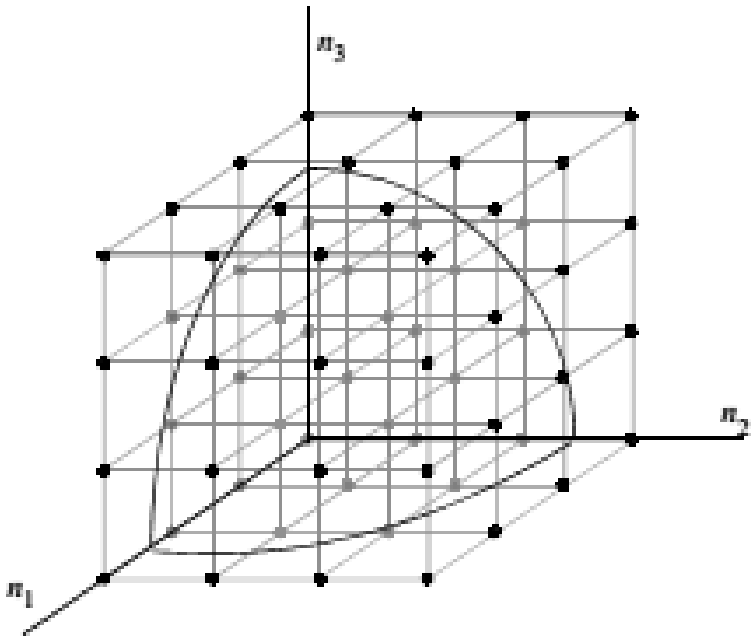

Fig 1.8: When a particle is enclosed in cubical box of dimension L the energy levels are discrete[14].

Each energy state corresponds to a point in three-dimensional (n_1, n_2, n_3)space in the positive octant. The spacing between the successive energy levels can be made as small as desired by choosing *L* sufficiently large [16].

1.2 Study Material: Calcium And Strontium

Calcium is a chemical element with the symbol Ca and atomic number 20. As an alkaline earth metal, calcium is a reactive metal that forms a dark oxide-nitride layer when exposed to air. Its physical and chemical properties are most similar to its heavier homologues strontium and barium. Calcium is a very ductile silvery metal (sometimes described as pale yellow) whose properties are very similar to the heavier elements in its group, strontium, barium, and radium. Like the other elements placed in group 2 of the periodic table, calcium has two valence electrons in the outermost s-orbital, which are very easily lost in chemical reactions to form a dipositive ion with the stable electron configuration of a noble gas, in this case argon. Hence, calcium is almost always divalent in its compounds, which are usually ionic. It is the fifth most abundant element in Earth's crust and the third most abundant metal, after iron and aluminium.

Calcium, strontium, barium, and radium are always considered to be alkaline earth metals; the lighter beryllium and magnesium, also in group 2 of the periodic table, are often included as well.

Some calcium compounds were known to the ancients, though their chemistry was unknown until the seventeenth century. Pure calcium was isolated in 1808 via electrolysis of its oxide by Humphry Davy, who named the element. Calcium compounds are widely used in many industries: in foods and pharmaceuticals for calcium supplementation, in the paper industry as bleaches, as components in cement and electrical insulators, and in the manufacture of soaps. On the other hand, the metal in pure form has few applications due to its high reactivity; still, in small quantities it is often used as an alloying component in steelmaking, and sometimes, as a calcium–lead alloy, in making automotive batteries.

The chemistry of calcium is that of a typical heavy alkaline earth metal. For example, calcium spontaneously reacts with water more quickly than magnesium and less quickly than strontium to produce calcium hydroxide and hydrogen gas. It also reacts with the oxygen and nitrogen in the air to form a mixture of calcium oxide and calcium nitrate.

Natural calcium is a mixture of five stable isotopes (40Ca, 42Ca, 43Ca, 44Ca, and 46Ca) and one isotope with a half-life so long that it can be considered stable for all practical purposes (48Ca, with a half-life of about 4.3 × 1019 years). Calcium is the first (lightest) element to have six naturally occurring isotopes.[17]

By far the most common isotope of calcium in nature is 40Ca, which makes up 96.941% of all natural calcium. It is produced in the silicon-burning process from fusion of alpha particles and is the heaviest stable nuclide with equal proton and neutron numbers; its occurrence is also supplemented slowly by the decay of primordial 40K. The other four natural isotopes, 42Ca,

43Ca, 46Ca, and 48Ca, are significantly rarer, each comprising less than 1% of all natural calcium. The four lighter isotopes are mainly products of the oxygen-burning and silicon-burning processes, leaving the two heavier ones to be produced via neutron capture processes.

Calcium cycling provides a link between tectonics, climate, and the carbon cycle. In the simplest terms, uplift of mountains exposes calcium-bearing rocks to chemical weathering and releases $Ca2+$ into surface water. These ions are transported to the ocean where they react with dissolved $CO2$ to form limestone ($CaCO3$), which in turn settles to the sea floor where it is incorporated into new rocks. Dissolved $CO2$, along with carbonate and bicarbonate ions, are termed "dissolved inorganic carbon" (DIC).[18]

The actual reaction is more complicated and involves the bicarbonate ion ($HCO{-}3$) that forms when $CO2$ reacts with water at seawater pH:

$$Ca2{+}{+} + 2HCO3 \rightarrow CaCO3(s) + CO2 + H2O$$

At seawater pH, most of the $CO2$ is immediately converted back into HCO-3. The reaction results in a net transport of one molecule of $CO2$ from the ocean/atmosphere into the lithosphere.[19] The result is that each $Ca2+$ ion released by chemical weathering ultimately removes one $CO2$ molecule from the surficial system (atmosphere, ocean, soils and living organisms), storing it in carbonate rocks where it is likely to stay for hundreds of millions of years.

Strontium

Strontium is the chemical element with the symbol Sr and atomic number 38. An alkaline earth metal, strontium is a soft silver-white yellowish metallic element that is highly chemically reactive. The metal forms a dark oxide layer when it is exposed to air. Strontium has physical and chemical properties similar to those of its two vertical neighbors in the periodic table, calcium and barium. It occurs naturally mainly in the minerals celestine and strontianite, and is mostly mined from these.

Natural strontium (isotope strontium-88) is stable, the synthetic strontium-90 is radioactive and is one of the most dangerous components of nuclear fallout, as strontium is absorbed by the body in a similar manner to calcium. Natural stable strontium, on the other hand, is not hazardous to health.

Because of its extreme reactivity with oxygen and water, strontium occurs naturally only in compounds with other elements, such as in the minerals strontianite and celestine. It is kept under a liquid hydrocarbon such as mineral oil or kerosene to prevent oxidation; freshly exposed strontium metal rapidly turns a yellowish color with the formation of the oxide.

Natural strontium is a mixture of four stable isotopes: 84Sr, 86Sr, 87Sr, and 88Sr.[19] Their abundance increases with increasing mass number and the heaviest, 88Sr, makes up about 82.6% of all natural strontium, though the abundance varies due to the production of radiogenic 87Sr as the daughter of long-lived beta-decaying 87Rb.[20] Of the unstable isotopes, the primary decay mode of the isotopes lighter than 85Sr is electron capture or positron emission to isotopes of rubidium, and that of the isotopes heavier than 88Sr is electron emission to isotopes of yttrium.

Applications

Cathodic monitor front panel made from strontium and barium oxide-containing glass. This application used to consume most of the world's production of strontium.

Consuming 75% of production, the primary use for strontium was in glass for colour television cathode ray tubes,[21] where it prevented X-ray emission.[22][23] This application for strontium has been declining because CRTs are being replaced by other display methods. All parts of the CRT must absorb X-rays. In the neck and the funnel of the tube, lead glass is used for this purpose, but this type of glass shows a browning effect due to the interaction of the X-rays with the glass. Therefore, the front panel is made from a different glass mixture with strontium and barium to absorb the X-rays.

Because strontium is so similar to calcium, it is incorporated in the bone. All four stable isotopes are incorporated, in roughly the same proportions they are found in nature. However, the actual distribution of the isotopes tends to vary greatly from one geographical location to another. Thus, analyzing the bone used to track animal migrations.[24][25]

Strontium chloride is sometimes used in toothpastes for sensitive teeth. One popular brand includes 10% total strontium chloride hexahydrate by weight.[26] Small amounts are used in the refining of zinc to remove small amounts of lead impurities.[27]

The drug strontium ranelate aids bone growth, increases bone density, and lessens the incidence of vertebral, peripheral, and hip fractures.[27][28] However, strontium ranelate also increases the risk of venous thromboembolism, pulmonary embolism, and serious cardiovascular disorders, including myocardial infarction. Its use is therefore now restricted.[29] Its beneficial effects are also questionable, since the increased bone density is partially caused by the increased density of strontium over the calcium which it replaces. Strontium also bio accumulates in the body.[30] Despite restrictions on strontium ranelate, strontium is still contained in some supplements.[31][32]

1.2.1 Crystal Structure

The face centered cubic structure has atoms located at each of the corners and the centers of all the cubic faces (left image below). Each of the corner atoms is the corner of another cube so the corner atoms are shared among eight unit cells. Additionally, each of its six face centered atoms is shared with an adjacent atom. Since 12 of its atoms are shared, it is said to have a coordination number of 12. The fcc unit cell consists of a net total of four atoms; eight eighths from corners atoms and six halves of the face atoms as shown in the middle image above. The image below highlights a unit cell in a larger section of the lattice.

In the fcc structure (and the hcp structure) the atoms can pack closer together than they can in the bcc structure. The atoms from one layer nest themselves in the empty space between the atoms of the adjacent layer. To picture packing arrangement, imagine a box filled with a layer of balls that are aligned in columns and rows. When a few additional balls are tossed in the box, they will not balance directly on top of the balls in the first layer but instead will come to rest in the pocket created between four balls of the bottom layer. As more balls are added they will pack together to fill up all the pockets. The packing factor (the volume of atoms in a cell per the total volume of a cell) is 0.74 for fcc crystals. Some of the metals that have the fcc structure include aluminum, copper, gold, iridium, lead, nickel, platinum and silver.

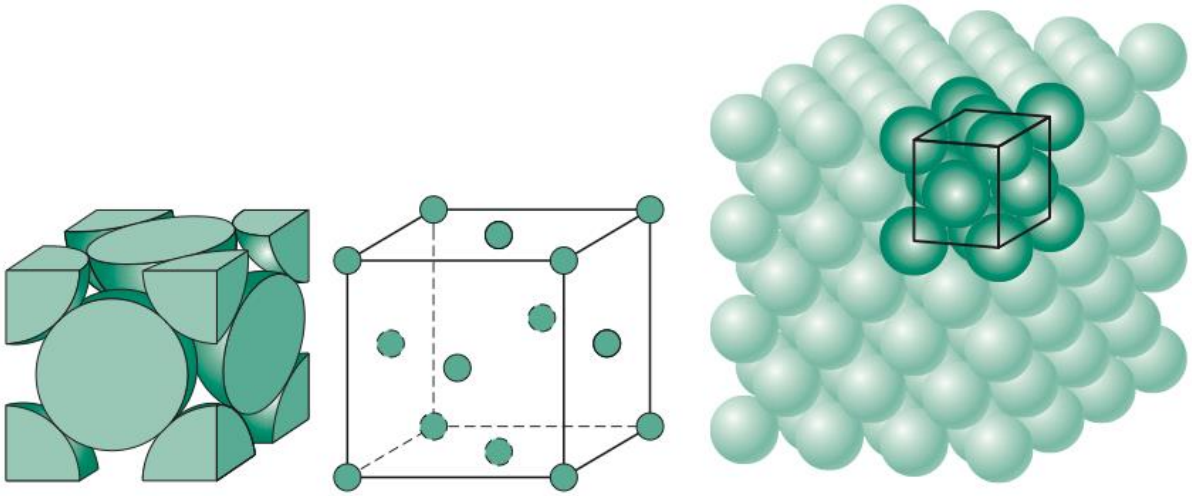

Fig. 1.9: Crystal structure of fcc phase[15].

1.2.2 Scope of The Present Work

The study of properties of solid is one of the most interesting and fruitful branches of physics. By knowing the lattice dynamics, we can predict different physical properties of solid and help to uses these solid in daily life application, which we can easily observed in this time period.

In this present work, we have studies the density of state (DOS) of alkaline earth metal Calcium and Strontium. From the study of DOS, we can get idea about nature of the solid and magnetic properties.

The main objective of our study are:

1. To study about the crystal structure done by previous worker.

2. To estimate the lattice parameter of Ca and Sr.

3. To study and plot the density of state of Ca and Sr.

1.3 How we Approach?

Mainly this research work is done is computational by using Quantum ESPRESSO (QE) package. First, we optimized structure of Alkaline earth metal by optimizing lattice parameters, then we study the band structure, DOS and PDOS of Calcium And Strontium. In this study,we choose Face-Centered structure because of its computational cost and simplicity of structure.

The outline of the present work is summarised follows:

In this work, Chapter 1 includes general introduction about crystal structure and lattice dynamics with attachment of objective and scope of work. In chapter 2, we discuss the theoretical models of the method employed in calculations such as Born-Oppenheimer, Hartree-Fock method, Density functional theory with local density approximation (LDA), General gradient approximation (GGA) and Pseudopotential. In chapter 3 we described some detail about Quantum ESPRESSO and its execution. Then in chapter 4 we discuss and present about main finding of this research. Finally, in chapter 5 we summarize our results and mention about further advantage of same field research. Reference are listed at end of chapter 5.

CHAPTER 2

LITERATURE REVIEW

Calcium along with its congeners magnesium, strontium, and Barium was first isolated by Humphy Davy in 1808.

M Tegze and J Hafner(1989) was calculated The electronic structure of calcium by means of the self-consistent linear combination of Gaussian orbitals method and the local-density approximation (LDA).They found that no shape approximations to charge density or the potential are made. They obtain a band structure and a Fermi surface which is in reasonble agreement with experiment.For that reason they disagree with the conclusions drawn in a paper submited by Jan and Skriver, who employed the linear muffin-tin orbital method and stated that the LDA cannot give a reasonable Fermi Surface. Their empty d-band width is somewhat narrower in comparison with other calculations or experiment.[33]

In 1989 Self-consistent calculations of the electronic structure of crystalline and amorphous Ca-Zn alloys using a linearised muffin-tin orbital super cell method. Strong similarities between the electronic densities of state of the metallic glasses and the corresponding crystalline compounds are found. This supports previous conclusions from molecular dynamics studies of the atomic structure that the local order in the metallic glasses is similar to that in the trigonal prismatic inter-metallic compounds. In the Ca-rich phases the s,p conduction band splits into a fully occupied Zn 4s band and a valence band that is of pure 4p character on the Zn sites and of a strongly s,p,d-hybridised character on the Ca sites. The consequences of this result for the chemical bonding and the electronic properties are discussed. Structural and electronic properties of crystalline and glassy calcium-zinc compounds.[34]

S. chatterjee and D.K. Chakrabarti in 2000 have been made to apply the `quantum defect method', in conjunction with the `composite wave variational method', to compute the band structure of divalent metals calcium, strontium and barium.[35] Also The quantum defect data have been deduced from experimental spectroscopic eigenvalues of singly-ionized Ca, Sr and Ba. They explained that The presence of an extra electron in each atomic cell has been taken into account by assuming a uniform charge density which produces a potential -2Z/r - Zr 2/r 3 s, r s being the radius of the Wigner-Seitz cell and Z being the valency of the metal. They performed the calculation of the band for all these metals neglecting - Zr 2/r 3 s. Then attempt has been made to take into account the term - Zr 2/r 3 s in the case of Ca. Both these calculations show that the Fermi surface of Ca is dismembered around the symmetry point W inside the Brillouin zone.

In 2007 Julia F. Medveda Emily N. Teasley Michael Haffman was performed First-principles electronic band structure investigations of five compounds of the CaO- Al2O3 family, 3CaO·Al2O3, 12CaO·7Al2O3, CaO·Al2O3, CaO·2Al2O3, and CaO·6Al2O3, as well as CaO and α-, θ-, and κ- Al2O3 [36]. They found that the conduction band in the complex oxides is formed from the oxygen anti bonding p states and, although the band gap in Al2O3 is almost twice larger than in CaO, the s states of both cations. Such a hybrid nature of the conduction band leads to isotropic electron effective masses which are nearly the same for all compounds investigated. This insensitivity of the effective mass to variations in the composition and structure suggested that upon a proper degenerate doping, both amorphous and crystalline phases of the materials will possess mobile extra electrons.

Wiley-vch Verlag Gmbh &Co KGaA Weinheim in 2004 presented the results of a first-principles study of the electronic and structural properties of strontium chalcogenides, SrS, SrSe and SrTe.[37] Their computational method is based on the full-potential linear muffin-tin orbitals

method(FP-LMTO) augmented by a plane-wave basis(PLW).Exchange and corrolation energy is described in local density approximation (LDA) using the perdew-Wang paramagnetization including a generalized gradient approximation(GGA). Their calculated results of the structural properties are given for the NaCl(B1) and CsCl(B2) structures.They had also carried out band-structure calculations for the three considered compound, but only for the three NaCl(B1) structure.A reasonable agreement is found from the comparison of their results with other theoretical calculations and experiment data.

VM Zainullinna, M.A Korotin & V.L Kozhevnikov was calculated the electronic structure of strontium ferrite $Sr_3Fe_2O_6$ using the tight-binding linear muffin-tin orbital method (TB LMTO) in the local spin density approximation of density functional theory with Coulomb correlations correction (LSDA+U).[38] Found that the semiconducting character of the spectrum with charge transfer energy gap of 1.82 eV was obtained in reasonably good agreement with experimental data. The iron ions are found to be in the high spin state. The calculated value of the local spin magnetic moment of Fe^{3+} ion is 3.94 μB which is not typical for trivalent iron ion in the high spin state. It is shown that the strong hybridization between Fe3d and O2p orbitals favors the $d^6\underline{L}$ configuration of Fe^{3+} ion, where $\underline{L}$ is a hole in the oxygen p shell. The mechanism of oxygen transport in ferrite is discussed basing on the total energy calculations of the different spatial configurations of oxygen vacancies.

CHAPTER 3

THEORY

3.1 General consideration

Determination of the electronic structure of solids is a many-body problem that requires the Schrödinger equation to be solved for an enormous number of nuclei and electrons. Even if we managed to solve the equation and find the complete wave function of a crystal, we face, the not less complicated problem of determining how this function should be applied to the calculation of physically observable values. While the exact solution of the many-body problem is impossible, it is also quite unnecessary.

3.2 Born-Oppenheimer approximation

To describe the various motions of the molecule we begin with the Schrodinger equation. The Hamiltonian is given by

$$H\hat{} = T\hat{}_e + T\hat{}_N + V_{ee} + V_{eN} + V_{NN}, \tag{3.1.1}$$

Where

$$T\hat{}_e = \sum_{i=1}^{N} \frac{p\hat{}_i^2}{2m} \tag{3.1.2}$$

represents the kinetic energy of the electrons and

$$T\hat{}_N = \sum_{v=1}^{2} \frac{p\hat{}_v^2}{2M_v} \tag{3.1.3}$$

is the kinetic energy of the nuclei. V_{eN} represents the attractive electron-nuclei potential. V_{ee} describes the repelling electron-electron interaction. V_{NN} indicates the repelling Coulomb interaction between the nuclei. Since the masses of the nuclei are very large,$T\hat{}_N$ can be neglected. This step is called the Born-Oppenheimer approximation. In the following, we will explain the approximation in more detail.

If we neglect the kinetic energy $T\hat{}_N$ of the nuclei (static approximation: fixed distance R of the nuclei), the relative distance R between the nuclei only occurs as a parameter. The Schrodinger equation becomes

$$[e + V_{ee}(r) + V_{eN}(r,R)]\varphi_n(r,R) = [\varepsilon_n(R) - V_{NN}(R)]\varphi_m(r,R). \qquad (3.1.4)$$

Here r indicates the position of the electron. The solutions $\varphi_n(r,R)$ depend parametrically on the distance between the nuclei. The energy of this state is given by the electronic energy $\varepsilon_n(R)$ lowered by $V_{NN}(R)$. The solutions $\varphi_n(r,R)$ represent a complete set of functions. The true wave function $\psi(r,R)$ can be expanded within this set:

$$\psi(r,R) = \sum_m \quad \phi_m(R)\varphi_n(r,R). \qquad (3.1.5)$$

The coefficients $\phi_m(R)$ are to be found and, in general, depend on R. $\varphi_n(r,R)$ is the solution of the full Schrodinger equation, which takes into consideration the kinetic energy $T\hat{}_N$ of the atomic nuclei, i.e.

$$(e + T\hat{}_N + V_{ee} + V_{eN} + V_{NN})\psi(r,R) = E\psi(r,R) \qquad (3.1.6)$$

Inserting (2.1.5) into (2.1.6) and using (2.1.4), we obtain

$$\sum_m \quad (\varepsilon_m(R) + T\hat{}_N)\phi_m(R)\varphi_n(r,R) = E\sum_m \quad \phi_m(R)\varphi_m(r,R) \qquad (2.1.7)$$

Now we multiply from the left-hand side with $\varphi^{\dagger}{}_n(r,R)$, integrate over the full space, and get

$$\sum_m \quad \int \quad \int \quad d^3r\varphi^{\dagger}{}_n(r,R)T\hat{}_N\phi_m(R)\varphi_m(r,R) + \varepsilon_m(R)\phi_n(R) = E\phi_n(R). \qquad (3.1.8)$$

Here we have used the orthogonality of the functions$\varphi_m(r,R)$. $T\hat{}_N$ is proportional to the Laplace operator Δ_R, which acts on $\varphi_m\varphi_m$. It holds that

$$\Delta_R(\phi\varphi) = (\Delta_R\phi)\varphi + 2\Delta_R\Phi.\Delta_R\varphi + \phi\Delta_R\varphi. \qquad (3.1.9)$$

The index R indicates the action of the operators in R space. The first term in (3.1.9) is proportional to $T\hat{}_N\phi_n$. The rest is brought to the right-hand side of (2.1.8). The result reads

$$[T\hat{}_N + \varepsilon_n(R)]\phi_n(R) = E\phi_n(R) - \sum_m \quad C_{nm}\phi_m(R) \qquad (3.1.10a)$$

With

$$C_{nm}\phi_m(R) = -\hbar^2 \sum_{\alpha} \quad \frac{1}{2M_\alpha} \int \qquad d^3r \varphi^{\dagger}{}_n(r,R) \times$$

$$\left[2\nabla_{R_\alpha}\phi_m(R).\nabla_{R_\alpha}\varphi_m(r,R) + \phi_m(R)\nabla_{R_\alpha}\varphi_m(r,R)\right]. \quad (3.1.10b)$$

The sum over a comes from $T\hat{}_N$ and ∇_{R_α}acts only on the co-ordinateR_α of the nucleus α, which appears in $R = \sqrt{(R_2 - R_1)^2}$. Now, the order of magnitude of C_{nm} is $\left(\frac{m}{M}\right)^{\frac{1}{2}}$times smaller than the electronic kinetic energy. This can be seen as follows. The order of magnitude of the term ~ $\hbar^2\nabla_{R_\alpha}\frac{\varphi_m}{2M_\alpha}$ (the kinetic energy of the nucleus) is proportional to $-\left(\frac{m}{M_\alpha}\right)\hbar^2\left(\nabla_r \frac{\varphi_m}{2} m\right)$; we have simply replaced ∇_{R_α} by ∇_r and introduced the electronic kinetic energy $\hbar^2\nabla_{R_\alpha}\frac{\varphi_m}{2M_\alpha}$. The factor m/Ma indicates that the contribution of ∇_{R_α} to C_{nm} is smaller by this factor than the kinetic energy of the electron.

The first term in (3.1.10b) remains to be estimated. For this we approximate ϕ_m by a harmonic oscillator wave function: $\phi_m \approx exp$,R_0 being the equilibrium position of nucleus α. We have

$$\nabla_{R_\sigma}\phi_m \approx |R - R_0|\frac{M\omega}{\hbar}\phi_m \approx \frac{(\delta R)M\omega}{\hbar}\phi_m \quad (3.1.11)$$

δRindicates the shift from the equilibrium position. The factor *M* is canceled by *1/M* in (2.1.10b) and the contribution is proportional to the vibrational energy$\hbar\omega$. As noted earlier, this goes like ~ $\left(\frac{m}{M}\right)^{\frac{1}{2}}$. As a summary, the C_{nm} term can be neglected or treated with the help of perturbation theory. Without the C_{nm} term, (2.1.10a) reduces to

$$[T\hat{}_N + \varepsilon_n(R)]\phi_n(R) = E\phi_n(R) \quad (3.1.12)$$

This equation has an interesting interpretation: the energy of the electron states $\varepsilon_n(R)$ acts like an effective potential in *R*. We imagine that the electrons build a "medium" in which the atomic nuclei move. This medium acts as an elastic band. If the nuclei try to leave the equilibrium position, they will be drawn back. There is an equilibrium position where $\varepsilon(R)$ has a minimum

deep enough to generate binding. The elastic band behaviour is then nothing other than the expansion up to the order $(R - R_0)^2$.

The C_{nm} produce a mixing between different statesφ_n and φ_m. This mixing between the $\varphi_n(R)$ states can be neglected in lowest order, because the C_{nm} are small [of order $\left(\frac{m}{M}\right)^{\frac{1}{2}}$, as explained previously]. Accordingly, the wave function is approximately given by

$$\psi_{nv}(r, R) = \phi_{nv}(R)\varphi_n(r, R) \tag{3.1.13}$$

Here *v* stands for all quantum numbers of level *n*. E_{nv} indicates the energy of the molecule, which is calculated from (3.1.12).

In order to describe vibrations and rotations of the molecule $\varepsilon_n(R)$ is expanded in coordinates describing vibration and rotation, respectively. The expansion in$\delta R = |R - R_0|$ up to the squared order leads to a harmonic vibrational potential (see Fig. 3.1). $\varepsilon_N(R)$does not depend on the angles (Euler angles). Hence the rotations of the molecule are free. An excitation of the molecule is a combination of excitations of the harmonic vibrational oscillator and of the rotations.

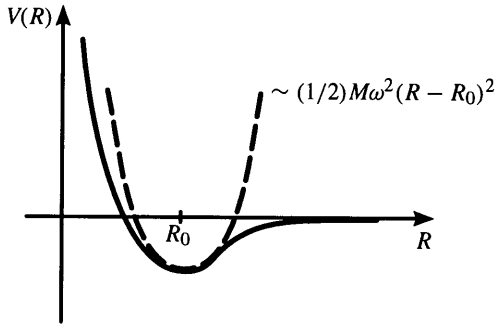

Fig. 3.1: Typical molecular potential for the nuclei in the molecule. *Ro* characterizes the relative equilibrium position of the two nuclei. R represents the relative nuclear distance

We summarize: in the Born-Oppenheimer approximation, first the energy levels of the electrons are determined for fixed distances *R* of the nuclear centers. The electron energy $\varepsilon_n(R)$plays the role of a potential, in which the nuclei are moving. If this potential has one or several deep

enough minima, one or several bound states of the molecule can exist. If the minima are only weak or do not exist at all, then the molecule is not bound.

3.3 Hartree-Fock Approximation

The simplest approach is to assume a specific form for the many-body wave function which would be appropriate if the electrons were non-interacting particles, namely

$$\psi^H(\{r_i\}) = \phi_1(r_1)\phi_2(r_2) \dots\dots \phi_N(N) \tag{3.1.14}$$

with the index i running over all electrons. The wave functions $\phi_i(r_i)$ are states in which the individual electrons would be if this were a realistic approximation. These are single-particle states, normalized to unity. This is known as the Hartree approximation (hence the superscript H). With this approximation, the total energy of the system becomes

$$E^H = \langle \Psi^H | H | \Psi^H \rangle$$

$$\sum_i \quad \langle \phi_i \left| \frac{-\hbar^2 \nabla_r^2}{2m_e} + V_{ion}(r) \right| \phi_i \rangle + \frac{e^2}{2} \sum_{ij(j\neq i)} \tag{3.1.15}$$

Using a variational argument, we obtain from this the single-particle Hartree equations:

$$\left[\frac{-\hbar^2 \nabla_r^2}{2m_e} + V_{ion}(r) + e^2 \sum_{j\neq i} \quad \langle \phi_j \vee \frac{1}{|r-r'|} \phi_j \rangle \right] \phi_i(r) + \epsilon_i \phi_i(r) \tag{3.1.16}$$

where the constants $\epsilon_i$are Lagrange multipliers introduced to take into account the normalization of the single-particle states ϕ_i(the bra $\phi_i \vee$ and ket $|\phi_i >$notation for single-particle states). Each orbital $\phi_i(r)$ can then be determined by solving the corresponding single-particle Schrödinger equation, if all the other orbitals $\phi_j(r_j), j \neq i$were known. In principle, this problem of self-consistency, i.e. the fact that the equation for one $\phi_i$depends on all the other ϕ_j's, can be solved iteratively. We assume a set of ϕ_i's, use these to construct the single-particle hamiltonian, which allows us to solve the equations for each new ϕ_i we then compare the resulting ϕ_i's with the original ones, and modify the original ϕ_i's so that they resemble more the new ϕ_i's. This cycle is continued until input and output ϕ_i's are the same up to a toleranceδ_{tol}, as illustrated in Fig. 3.2 (in this example, the comparison of input and output wave functions is made through the

densities, as would be natural in Density Functional Theory, discussed below). The more important problem is to determine how realistic the solution is. We can make the original trial ϕ's orthogonal, and maintain the orthogonality at each cycle of the self-consistency iteration to make sure the final ϕ's are also orthogonal. Then we would have a set of orbitals that would look like single particles, each $\phi_i(r)$ experiencing the ionic potential $V_{ion}(r)$ as well as a potential due to the presence of all other electrons, $V_i^H(r)$given by

$$V_i^H(r) = +e^2 \sum_{j\neq i} \quad \langle \phi_j \vee \frac{1}{|r-r'|} \phi_j \rangle \tag{3.1.17}$$

1. Choose $\phi_i^{(in)}(\mathbf{r})$

↓

2. Construct $\rho^{(in)}(\mathbf{r}) = \sum_i |\phi_i^{(in)}(\mathbf{r})|^2$, $V^{sp}(\mathbf{r}, \rho^{(in)}(\mathbf{r}))$

↓

3. Solve $\left[-\frac{\hbar^2}{2m_e}\nabla_{\mathbf{r}}^2 + V^{sp}(\mathbf{r}, \rho^{(in)}(\mathbf{r}))\right] \phi_i^{(out)}(\mathbf{r}) = \epsilon_i^{(out)} \phi_i^{(out)}(\mathbf{r})$

↓

4. Construct $\rho^{(out)}(\mathbf{r}) = \sum_i |\phi_i^{(out)}(\mathbf{r})|^2$

↓

5. Compare $\rho^{(out)}(\mathbf{r})$ to $\rho^{(in)}(\mathbf{r})$

If $|\rho^{(in)}(\mathbf{r}) - \rho^{(out)}(\mathbf{r})| < \delta_{tol} \rightarrow$ STOP; else $\phi_i^{(in)}(\mathbf{r}) = \phi_i^{(out)}(\mathbf{r})$, GOTO 2.

Figure 3.2: Schematic representation of iterative solution of coupled single-particle equations. This kind of operation is easily implemented on the computer.

This is known as the Hartree potential and includes only the Coulomb repulsion between electrons. The potential is different for each particle. It is a mean-field approximation to the electron–electron interaction, taking into account the electronic charge only, which is a severe simplification [30].

3.4 Density functional theory

There are numerous fields inside the physical sciences and building where the way to scientific and mechanical advancement is understanding and controlling the properties of issue at the degree of individual iotas and particles. Thickness utilitarian hypothesis is an incredibly fruitful way to deal with finding answers for the essential condition that depicts the quantum conduct of ion as and atoms, the Schrödinger condition, in settings of down to earth esteem. This methodology has quickly developed from being a specific workmanship rehearsed by few physicists and scientific experts at the front line of quantum mechanical hypothesis to a device that is utilized normally by huge quantities of analysts in science, material science, materials science, substance building, topography, and different controls. A hunt of the Science Citation Index for articles distributed in 1986 with the words "thickness useful hypothesis" in the title or dynamic yields under 50 passages. Rehashing this quest for 1996 and 2006 gives more than 1100 and 5600 passages, separately [31]. Right now, start an audit of some key thoughts from quantum mechanics that underlie DFT (and different types of computational science).

The whole field of thickness useful hypothesis lays on two basic numerical hypotheses demonstrated by Kohn and Hohenberg and the inference of a lot of conditions by Kohn and Sham in the mid-1960s [31].The first theorem,proved by Hohenberg and Kohn, is: The ground-state vitality from Schrödinger's condition is a one of a kind utilitarian of the electron thickness.

Tragically, in spite of the fact that the first Hohenberg–Kohn hypothesis thoroughly demonstrates that a practical of the electron thickness exists that can be utilized to tackle the Schrödinger condition, the hypothesis says nothing regarding what the utilitarian really is. The second Hohenberg–Kohn hypothesis defines a significant property of the practical: The electron thickness that limits the vitality of the general utilitarian is the genuine electron thickness comparing to the full arrangement of the Schrödinger condition. In the event that the "genuine" utilitarian structure were known, at that point we could fluctuate the electron thickness until the

vitality from the practical is limited, giving us a solution for finding the significant electron thickness. This variational guideline is utilized by and by with surmised types of the useful.

3.5 The Kohn-Sham approach

While the Hohenberg–Kohn theorem rigorously establishes that we may use the density, and and therefore the density alone, as a variable to find the ground-state energy of an N-electron problem, it does not provide us with any useful computational scheme. This is provided by the Kohn–Sham formalism. Let us then start by considering a noninteracting *N*-electron system in an external potential V_s. The Hamiltonian H_s of this system is given by

$$H_s = T + V_s \tag{3.1.18}$$

We then apply the Hohenberg–Kohn theorem to the present system. Accordingly, there exists a unique energy functional

$$\mathcal{E}_s[n] = T[n] + \int V_s(r)n(r)\,dr \tag{3.1.19}$$

We note here that $T_s[n]$ is the kinetic energy functional of a system of N non interacting electrons. The ground-state density of this system is easily obtained. It is simply

$$n_s(r) = \sum_{i=1}^{N} \quad |\phi_i(r)|^2 \tag{3.1.20}$$

where we have occupied the N single-particle states, or orbitals, that satisfy the Schrödinger-like equation

$$\left[\frac{-\hbar^2}{2m}\nabla^2 + V_s\right]\phi_i(r) = \mathcal{E}_i\phi_i(r), \mathcal{E}_1 \leq \mathcal{E}_2 \leq \mathcal{E}_3 \ldots, \tag{3.1.21}$$

and have the *N* lowest eigenvalues $\mathcal{E}_i$. But we are really interested in a system of *N* interacting electrons in an external potential V_{ext}, so the question we would like to answer is the following: can we determine the form that V_s (the external potential of the non interacting system) must take in order for the non interacting system to have the same ground-state density as the interacting system in the external potential V_{ext}? The strategy we use is to solve for the density using the auxiliary non interacting system, and then insert this density (which by construction is the same

as that for the interacting system) into an approximate expression for the total energy of the interacting system. The first step in this process is to rewrite the energy functional $\mathcal{E}[n]$ of the interacting system, which was given in Eq. (3.1.21), as

$$\mathcal{E}[n] = T_s[n] + \left\{T[n] - T_s[n] + V[n] - \frac{e^2}{2}\iint \frac{n(r)n(r')}{|r-r'|}drdr'\right\} + \frac{e^2}{2}\iint \frac{n(r)n(r')}{|r-r'|}drdr'$$

$$+ \int n(r)V_{ext}(r)dr$$

$$\equiv T_s + \frac{e^2}{2}\iint \frac{n(r)n(r')}{|r-r'|}drdr' + \iint n(r)V_{ext}(r)dr + \mathcal{E}_{XC}[n], \quad (3.1.22)$$

Here we have added and subtracted both the kinetic energy functional $T_s[n]$ of a non interacting system and the direct, or Hartree, term in the electrostatic energy. We have then defined the sum of the terms in braces to be the exchange-correlation energy functional $\mathcal{E}_{XC}[n]$ is

$$\mathcal{E}_{XC}[n] \equiv F_{HK}[n] - \frac{e^2}{2}\iint \frac{n(r)n(r')}{|r-r'|}drdr' - T_s[n], \quad (3.1.23)$$

We have thus swept all our ignorance about electron interactions beyond the Hartree term under the rug that we call $\mathcal{E}_{XC}[n]$. What we gain in writing $\mathcal{E}_{XC}[n]$ this way is that we can eventually focus on developing reasonable approximations for $\mathcal{E}_{XC}[n]$. According to the Hohenberg–Kohn theorem, the density n that minimizes the functional $\mathcal{E}[n]$ is the ground-state density. Thus, by taking the variation of Eq. (2.1.22) with respect to the particle density we obtain

$$\frac{\delta\mathcal{E}[n]}{\delta n(r)} = \frac{\delta T_s[n]}{\delta n(r)} = e^2\int \frac{n(r')}{|r-r'|}dr' + V_{ext}(r) + v_{xc}[n(r)] = 0, \quad (3.1.24)$$

where we have formally defined the exchange-correlation potential as

$$v_{xc}[n(r)] \equiv \frac{\delta\mathcal{E}_{xc}[n]}{\delta n(r)}.$$

We now use the auxiliary non interacting system and its Schrödinger equation, from which we are able to similarly show that

$$\frac{\delta T_s[n]}{\delta n(r)} + V_s(r) = 0.$$

By comparing this result with Eq. (2.5.6) we see that this ejective potential V_s (r) must satisfy

$$V_s(r) = V_{ext}(r) + e^2 \int \frac{n(r')}{|r-r'|} dr' + v_{xc}(r), \qquad (3.1.25)$$

We are now doing a position to implement the self-consistent Kohn–Sham scheme. We first choose an initial trial form of the function $n(\mathbf{r})$ and substitute into Eq. (3.1.25) to find a trial form of V_s. We then solve Eq. (3.1.19) for the single-particle wave functions$\phi_i(r)$, and use Eq. (3.1.18) to find the next iteration for $n(\mathbf{r})$. When this procedure has been repeated a sufficient number of times that no further changes occur, then a solution for $n(\mathbf{r})$ has been found that not only satisfies the Schrödinger equation for the reference noninteracting electrons, but also is the correct density for the interacting system. We close this section by highlighting a few points about the Kohn–Sham formalism. First of all, it is formally exact, supposing that we can find the exact exchange-correlation potential $v_{xc}(r)$. Second, we have cast the solution of the interacting *N*-electron problem in terms of non interacting electrons in an external potential $V_s(r)$. This is of great practical importance. The ground state wave function of the non interacting system is just a Slater determinant of the *N* orbitals, the so-called Kohn–Sham orbitals, with the lowest eigenvalues E. It is relatively easy to unravel for these single-particle orbitals even for as many as a couple of hundred electrons [32]. The Kohn–Sham equations formally look considerably like self-consistent Hartree equations, the only difference being the presence of the exchange-correlation potential. This makes them much simpler to solve than the Hartree–Fock equations, in which the potential is orbital-dependent. In the Kohn–Sham and Hartree equations, the effective potential is the same for every orbital.

3.6 The Local Density Approximation

In band calculations, usually certain approximations for the exchange–correlation potential $V_{xc}(r)$ are used. The simplest and most frequently used is the local density approximation (LDA), where $\rho_{xc}(r, r'-r)$a form similar to that for a homogeneous electron has gas, but with the density at every point of the space replaced by the local value of the charge density, $\rho(r)$for the actual system:

$$\rho_{xc}(r, r'-r) = \rho(r) \int_0^2 \quad d\lambda g_0\big(r - r' \vee, \lambda, \rho(r)\big) - 1, \tag{3.1.26}$$

Where,g_0 is the pair correlation function of a homogeneous electron system. Substituting (3.1.26) into (3.1.27) we obtain the local density approximation [44]:

$$E_{xc}[\rho] = \int \rho(r)\varepsilon_{xc}(\rho)\, dr, \tag{3.1.27}$$

Here, ε_{xc} is the contribution of exchange and correlation to the total energy (per electron) of a homogeneous interacting electron gas with the density$\rho(r)$. This approximation corresponds to surrounding every electron by an exchange– correlation hole and must, as expected, be quite good when $\rho(r)$varies slowly. The DFT includes the exchange and correlation effects in a more natural way in comparison with Hartree-Fock-Slater method. Here, the exchange– correlation potential V_{xc} may be represented as

$$V_{xc}(r) = \beta(r_e)V_{GKS}(r), \tag{3.1.26}$$

where V_{GKS} is the Gaspar–Kohn–Sham potential, and r_e is given by

$$r_e(r) = \left[\frac{3}{4\pi}\rho(r)\right]^{\frac{1}{3}}. \tag{3.1.29}$$

This parameter corresponds, in order of magnitude, to the ratio of the potential energy of particles to their average kinetic energy

3.7 The Generalized Gradient approximation

An early endeavor to improve the LSDA was the inclination development estimation (GEA). Figurings for molecules and a jellium surface appeared, be that as it may, that the GEA doesn't improve the LSDA if the stomach muscle initio coefficients of the slope revision are utilized. The blunders in the GEA were examined by Langreth and Perdew and later by Perdew and colleagues. It was demonstrated that the second request developments of the trade and relationship openings in angles of the thickness are genuinely sensible near the electron, yet not far away. In the first work of Langreth and associates a summed up inclination guess (GGA) was developed by means of cut-off of the deceptive little wave-vector commitment to the Fourier change of the second request thickness angle extension for the trade relationship opening around an electron. Later Perdew and associates contended that the inclination developments can be made increasingly practical by means of genuine space shorts picked to authorize careful properties regarded by zero-request or LSD terms however abused constantly request extensions: The trade gap is rarely positive, and incorporates to - 1, while the relationship opening coordinates to zero. Various GGA plans were created by Langreth and Mehl, Hu and Langreth (LMH), Becke, Engel and Vosko, and Perdew and collaborators (PW), the three best and well known ones are those by Becke (B88), Perdew and Wang (PW91), and Perdew, Burke, and Ernzerhof (PBE). In GGA the trade relationship utilitarian of the electron turn densities $\rho_{\uparrow}$ and $\rho_{\downarrow}$ takes the form

$$E_{xc}^{GGA}[\rho_{\uparrow}, \rho_{\downarrow}] = \int \quad d^3 r f(\rho_{\uparrow}, \rho_{\downarrow}, \nabla\rho_{\uparrow}, \nabla\rho_{\downarrow}) \tag{3.1.30}$$

The GGA functionals were tried in a few cases, and were found to give improved outcomes for the ground-state properties. For iotas it was discovered that both all out energies and expulsion energies are improved in the LMH practical contrasted and the LSDA. The PW practical gives a further improvement in the all out vitality of iotas. The coupling energies of the first push diatomic atoms are additionally improved by both functionals. In an investigation of the band

structure of V and Cu, Norman and Koelling found that the LMH potential gave an improvement in the Fermi surface for V yet not for Cu. The strong vitality, the cross section parameters, and the mass modulus of third-push components have been determined utilizing the LMH, PW, and the angle extension functionals in. The PW practical was found to give to some degree preferred outcomes over the LMH utilitarian and both were found to commonly evacuate a large portion of the mistakes in the LSD estimate, while the GEA gives more terrible outcomes than neighborhood thickness guess. For Fe GGA functionals accurately anticipate a ferromagnetic bcc ground state, while the LSDA and the angle extension foresee a nonmagnetic FCC ground state. Likewise, the GGA amends LSDA underestimation of the cross section constants of Li and Na. Enormous number of test estimations demonstrated that GGA functionals yield incredible improvement over LSD in the portrayal of finite frameworks: they improve the complete energies of particles and the strong vitality, harmony separation, and vibrational recurrence of atoms, however have blended history of achievements and disappointments for solids. This might be on the grounds that the trade connection opening can have a diffuse tail in a strong, yet not in a particle or little atom, where the thickness itself is all around confined. The general pattern is that the GGA thinks little of the mass modulus and zone focus transverse optical phonon recurrence, remedies the coupling vitality, and amends or overcorrects, particularly for semiconductor frameworks, the cross section consistent contrasted with LDA. The GGA doesn't take care of the issues experienced in the change metal monoxides FeO, CoO, and NiO. The attractive minutes and band structures acquired with the GGA for the oxides are basically indistinguishable off base ones from got with the LSDA. As of late, various endeavors have been made to broaden the GGA by including higher request terms, specifically the Laplacian of the electron thickness, into the extension of the trade connection gap. Be that as it may, no broad trial of the nature of these new possibilities with application to solids have yet been made [32].

3.8 Pseudo-potentials

The key thought of "pseudopotential" is the supplanting of one issue with another. The essential application in electronic structure is to supplant the solid Coulomb capability of the core and the impacts of the firmly bound center electrons by a powerful ionic potential following up on the valence electrons. Pseudopotential can be created in a nuclear estimation and afterward used to process properties of valence electrons in atoms or solids, since the center states remain practically unaltered. Moreover, the way that pseudopotentials are not special permits the opportunity to pick shapes that disentangle the computations and the translation of the subsequent electronic structure. The approach of "stomach muscle initio standard saving" and "ultrasoft" pseudopotentials has prompted precise estimations that are the reason for a great part of the momentum innovative work of new techniques in electronic structure, as portrayed in the accompanying sections. A large number of the thoughts started in the orthogonalized plane wave (OPW) approach that throws the eigenvalue issue as far as a smooth piece of the valence capacities in addition to center (or center like) capacities. The OPW technique has been brought into the advanced system of all out vitality functionals by the projector increased wave (PAW) approach that utilizations pseudopotential administrators yet keeps the full center wavefunctions.

Norm-conserving pseudo potentials

Pseudo potentials generated by calculations on atoms (or atomic-like states) are termed "ab initio" because they are not fitted to experiment. The concept of "norm-conservation" has a special place in the development of ab initio pseudo potentials; at one stroke it simplifies the application of the pseudo potentials and it makes them more accurate and transferable. Norm-conserving pseudo functions$\psi_{ij}(r)$ are normalized and are solutions of a model potential chosen to reproduce the valence properties of an all electron calculation. In the application of the pseudo potential to complex systems, such as molecules, clusters, solids, etc., the valence pseudo functions satisfy the usual ortho normality conditions as

$$\langle \psi_i^{\sigma,PS} \vee \psi_i^{\sigma',PS} \rangle = \delta_{i,j}\delta_{\sigma,\sigma'} \tag{3.1.31}$$

so that for the Kohn-Sham equations have the same form as

$$\left(H_{KS}^{\sigma,PS} - e_i^{\sigma}\right)\psi_i^{\sigma,PS}(r) = 0 \tag{3.1.32}$$

Ultrasoft pseudopotential (USPP)

One goal of pseudo potentials is to create pseudo functions that are as "smooth" as possible, and yet are accurate. "Norm-conserving" pseudopotentials achieve the goal of accuracy, usually at some sacrifice of "smoothness."

A different approach known as "ultrasoft pseudopotentials" reaches the goal of accurate calculations by a transformation that re-expresses the problem in terms of a smooth function and an auxiliary function around each ion core that represents the rapidly varying part of the density. We will focus upon examples of states that present the greatest difficulties in the creation of accurate, smooth pseudofunctions: valence states at the beginning of an atomic shell, *Is,2p, 3d,* etc.

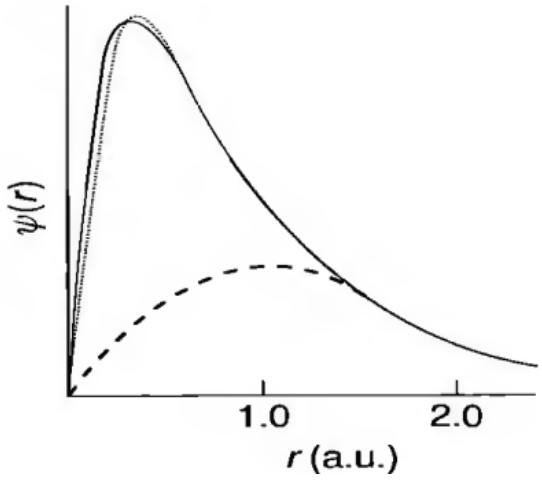

Figure 3.3: 2p radial wavefunction$\psi(r)$ for oxygen treated in the LDA, comparing the all-electron function (solid line), a pseudofunction generated using the Hamann approach (dotted line), and the smooth part of the pseudofunction$\psi\sim$ in the "ultrasoft" method (dashed line).

For these states, the OPW transformation has no effect since there are no core states of the same angular momentum. Thus, the wavefunctions are nodeless and extend into the core region. Accurate representation by norm-conserving pseudofunctions requires that they are at best only moderately smoother than the all-electron function (see Fig.3.3) The difference in the norm equation $Q_l = \int_0^{R_c} \quad dr\phi_l(r)^2$from that norm-conserving function $\phi = r\psi\sim$ (either an all-electron function or a pseudofunction) is given by

$$\Delta Q_{s,s\prime} = \int_0^{R_c} \quad dr\Delta Q_{s,s\prime}(r). \tag{3.1.33}$$

Where

$$\Delta Q_{s,s\prime}(r) = \phi_s\ (r)\phi_{s\prime}(r) - \phi\sim_s\ (r)\phi\sim_{s\prime}(r). \tag{3.1.34}$$

A new non-local potential that operates on the $y can now be defined to be

$$\delta V\hat{}_{NL}^{US} = \sum_{s,s\prime} \quad D_{s,s\prime} \vee \beta_s > \beta_{s\prime} \vee, \tag{3.1.35}$$

Where

$$D_{s,s\prime} = B_{s,s\prime}\varepsilon_{s\prime}\Delta Q_{s,s\prime}. \tag{3.1.36}$$

For each reference atomic states *s*, it is straightforward to show that the smooth functions $\psi\sim_s$are the solutions of the *generalized eigenvalue problem*

$$[H\hat{} - \varepsilon_s S\hat{}]\psi\sim_s = 0, \tag{3.1.37}$$

With$H\hat{} = \frac{-1}{2}\Delta^2 + V_{local} + \delta V\hat{}_{NL}^{US}$ and $S\hat{}$ an overlap operator,

$$S\hat{} = 1\hat{} + \sum_{s,s\prime} \quad \Delta Q_{s,s\prime}|\beta_s > \beta_{s\prime}|, \tag{3.1.38}$$

which is different from unity only inside the core radius. The eigenvalues ε_s agree with the all-electron calculation at as many energies s as desired. The full density can be constructed from the functions $\Delta Q_{s,s\prime}(r)$, which can be replaced by a smooth version of the all-electron density. The advantage of relaxing the norm-conservation condition $\Delta Q_{s,s\prime} = 0$ is that each smooth pseudofunction $\psi\sim_s$ can be formed independently, with only the constraint of matching the value of the functions $\psi\sim_s(R_c) = \psi_s(R_c)$ at the radius R_c. Thus, it becomes possible to

choose R_c much larger than for a norm-conserving pseudopotential, while maintaining the desired accuracy by adding the auxiliary functions $\Delta Q_{s,s'}(r)$ and the overlap operator S. An example of the un-normalized smooth function for the 2p state of oxygen is shown in Fig. 3.9.1, compared to a much more rapidly varying norm-conserving function [42]

3.9 Band Structure

If we knew the potential $V_P(r)$, and could solve the one-electron Schrödinger equation

$$(\frac{-\hbar^2}{2m_e}\nabla^2\psi(r) + V_P(r)\psi(r) = E\psi(r)$$

we could ascertain the energies E of the entirety of the different potential states. There are a few different ways of moving toward such figurings from first standards, and we won't go into those here. The after effects of such counts give what is known as a band structure. The electronic conditions of precious stones are portrayed by the band hypothesis of solids. The external orbital's of the molecules in a thickly stuffed strong cover with one another as the synthetic bonds that hold the gem together are framed. This causes the discrete vitality levels of the free ion as to be expanded into groups. The differentiation between a protector and a semiconductor is identified with the size of the band gap. Semiconductors have littler band holes than encasings. The free electrons in the conduction band can direct power effectively in a similar way as the free electrons in metals. Semiconductors, hence, have a higher conductivity than encasings, yet a littler conductivity than metals as a result of the modest number of free electrons [43]. There are various groups in a band structure (in actuality a limitless number), yet generally, just a couple are significant in deciding specific properties of a material. Fig. 8.4 outlines a basic band structure. Each band has an all out number of permitted k-states equivalent to the number of unit cells in the precious crystal.

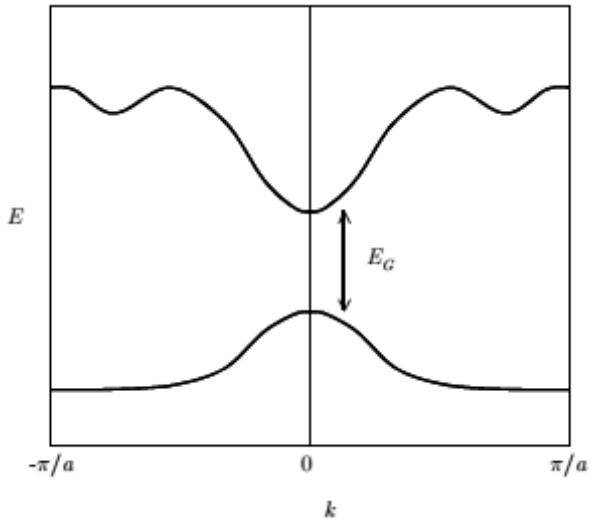

Fig. 3.4: Figurative illustration of a semiconductor band structure, plotted along one crystal direction. The upper "band" (line) will be essentially empty of electrons, and is called the conduction band; the lower band will be essentially full of electrons, and is called the valence band[44].

Fig. 3.4 illustrates a simplified band structure. In each band, we only have to plot *k*-values from $-\pi / a$ to π / a. The band structure in Fig. 3.4 is also drawn to be symmetric about $k = 0$. Band structures are often symmetric in this way. In our simple one-electron model, neglecting magnetic effects, the existence of symmetries like this is easily proved [45].

3.10 GW approximation

While we have given some justifications to utilizing a straight forward LSDA band structure way to deal with assessing excitation energies, various materials with intriguing attractive properties include firmly corresponded electronic states, and other estimated approaches have been created to go past the LSDA. For the quasiparticle issue, the focal issue is a sufficient estimation for the self-vitality administrator, $\Sigma_{GW}(r, r'; E)$. A working technique for tackling this issue is the purported GW estimation. On the off chance that the pinnacle is sufficiently sharp, well-defined quasiparticle vitality can be acquired. Where the self-energy is

$$\Sigma_{GW}(r, r'; t) = iG(r, r'; t)W(r, r': t) \tag{3.1.39}$$

The self-vitality in the GW A has a similar structure as that in the Hartree-Fock estimate aside from that it relies upon the vitality and contains a term that relies upon abandoned states as an outcome of relationship impacts. In this manner, the GW A can be deciphered as a speculation of the Hartree-Fock estimate with a potential that contains dynamical screening of the Coulomb potential. The GWA has been fruitful in treating the quasiparticle frameworks, for example, free-electron like metals and semiconductors It can be demonstrated that the GWA hypotheses might be identified with a Hartree-Fock hypothesis with a recurrence and orbital-subordinate screened Coulomb association and, at any rate for confined states, for example, d or f orbital's of progress metal or uncommon earth metal particles [46].

CHAPTER 4

COMPUTATIONAL DETAILS

4.1 General Consideration

In this chapter, we discuss details about our present work with the first principle pseudopotential-based density functional calculations including norm-conserving pseudo-potential in the DFT approach by using The quantum ESPRESSO (QE) computational package. Some practicable commands along with their functions are well detailed here.

4.2 Quantum Espresso Program

In this activity, you will use the Density Functional Theory (DFT) to investigate the properties of different materials. DFT is broadly utilized in industry, and in the scholastic research network since it is one of the computational techniques that can (roughly) tackle reasonable quantum mechanical issues numerically [24]. Quantum ESPRESSO-a condensing for Quantum Open-Source Package for Research in Electronic Structure, Simulation, and Optimization program is a multi-reason and multi-stage PC coding program for electronic-structure figurings and materials demonstrating. This bundle is essentially utilized in the stomach muscle ab-initio estimations of dense issue frameworks. In a controlled issue material science, its ordinary application in the stomach muscle ab-initio estimations like-basic advancements (both at zero and limited temperature), direct reaction computations (Phonons, flexible constants, dielectric, and some more) and so forth stretches out to high-temperature atomic elements. The significant element of the bundle remembered for the product are :

(i) Plane Wave self-consistent field (PWscf)

(ii) First-Principles Molecular Dynamics (FPMD) and

(iii) Car-Parrinello (CP). QE, based on DFT, implements a variety of methods and algorithms for a chemically realistic modelling of materials from the Nano-scale upwards

(iv) Chemical reactivity and transition-path sampling, using Nudged Elastic Band (NEB) method

(v) Computational microscopy (STM). This package uses a plane waves (PWs) basis set for the expansion of electronic wave function, a pseudopotentials (PPs) to represent electron-ion interactions and DFT for the description of electron-electron interaction.

Some basic computations/simulations that can be performed by this package include:

- Calculations of the Kohn-Sham (KS) orbitals and energies for isolated and extended systems, and of their ground states energies.
- Structural modelling (equilibrium structures of molecules, crystals, surfaces).
- Atomic forces and stresses.
- Ground state studies of magnetic or spin-polarized systems.
- Dynamical modeling (first-principles molecular dynamics) either in the electronic ground state (Born-Oppenheimer) or with fictitious electronic kinetic energy (Car-Parrinello).

Density-Functional Perturbation Theory (DFPT) used in the package to calculate the energy derivatives and related quantities. QE package are used as our first — principles code. QE is a full ab- initio package implementing electronic structure and energy calculation, linear response method (to calculate dielectric constants, Born effective charge and phonon dispersion curves) and third order an-harmonic perturbation theory. It also contains two molecular- dynamics codes, CPMD (Car-Parrinello Molecular Dynamics) and FPMD (First-Principles Molecular Dynamics). Among them, to perform the total energy calculations, PWscf code is used, which used both norm-conserving pseudopotential (PP) and Ultra soft Pseudo-potentials (US-PP)

within DFT. In our case, we use Quantum ESPRESSO integrated module of codes, based on DFT by using plane basis set for expansion of wave function and pseudopotential with required content in first-principle method of calculation to calculate total energies and optimize geometries of transition metal Ti and Zr. Also, by using this package, band structure is calculated and partial density of states (PDOS) is used to find the nature of material.

4.2.1 PWscf

PWscf stands for Plane Wave self-consistent field (which in earlier releases included PHonon and PostProc), developed by Stefano Baroni, Stefano de Gironcoli, Andrea Dal Corso (SISSA) Paolo Giannozzi (Univ. Udine), and many others [25]. PWscf implements an iterative approach for self-consistency, in the framework of the plane-wave pseudo potential method. This package uses the well-established LDA and GGA exchange-correlation functionals, including spin-polarizations. The main feature of PWscf calculation is the self-consistency calculations, structural relaxation, electronic structure calculations, variable cell molecular dynamics calculation, etc, performed by invoking executable file called pw.x. The structural optimization is performed using the Broyden-Fletcher-Goldfarb-Shanno (BFGS) [26].

Some of the most important parameters in the input file of the Quantum espresso are as indicated below.

- &CONTROL: general variables controlling the run
- &SYSTEM: structural information on the system under investigation · &ELECTRONS: electronic variables: self-consistency, smearing
- ibrav : 4, this keyword generates hexagonal closed pack (hcp) structure.
- celldm(1): specifies the lattice constant of the crystal and are usually given in atomic unit. · ecutwfc: kinetic energy cutoff (Ry) for wavefunctions (1 Ry=13.6ev).
- nat: number of atoms in the unit cell which is 2.

- ntyp: number of types of atoms in the unit cell.
- nbnd: represents the number of electronic stated (bands) to be calculated.
- Atomic Species: It specifies the symbols of the atoms, their corresponding masses (in amu) and the name of the files containing the pseudo-potentials.
- Atomic Positions: specifies the atomic co-ordinates of the atoms which are defined for the proper structure.
- k-points: represents the rectangular grid of points of dimensions, spaced evenly throughout the Brillouin zone and this keyword requires appropriate unit.

4.2.2 PostProcessing

The package called Postprocessing was Originally developed by Stefano Baroni, Stefano de Gironcoli, Andrea Dal Corso (SISSA), Paolo Giannozzi (Univ. Udine), and many others. After the Self Consistent calculation has been converged, we use many small calculations such as plotting of band, density of states (DOS) etc.

The main post processing codes which extract the specified data/files from the PWscf calculations and perform further calculations are as follows;

pw.x: We use this command to run the input files of scf and nscf calculations of energy and wave functions at each k-points, which extracts the output files for the energy calculation at every k-points.

bands.x : This extracts the files from PWscf calculation and records its eigenvalues at different K-points with corresponding energies values ready for further processing. The code bands.x also performs the symmetry analysis of the band structure.

plotband.x : The output file of bands.x is directly read and converted to plottable format by auxiliary code plotband.x. The value of k-points must be correctly put in a sequence, otherwise unpredictable plots may result if k-points are not in sequence along lines or if two consecutive points are same. Thus, proper choice of sequence of k-points is important.

dos.x : This code helps us to calculate the electronic density of states at different k-points.

projwfc.x : This code calculates projections of wave functions over atomic orbitals. It gives the contributions of the atomic orbitals s, p, d, f.

CHAPTER 5

RESULTS AND DISCUSSION

5.1 General Consideration

This thesis has describes the comparative study of element Calcium (Ca) and Strontium (Sr). One of the main challenges in first principle calculation is the geometric optimization of structures. We have taken out the energy minimization of Ca and Sr, followed by the study of electronic band structures and the density of states. The calculation has been carried out using density functional theory using generalized gradient approximation. At first, in the GGA method, energy minimization is done with respect to the lattice parameter then the same lattice parameter corresponding to the minimum energy state is used to carry out further calculations. In-band structure calculations, We plotted the graph of energy versus the high symmetry k-points and then analyzed the properties of the substance on the basis of band lines and bandgap. To view the individual contribution of different orbital electrons, we study the conduction band edge and valance band edge. Likewise, the Density of states (DOS) is performed to get information about the nature of the bandgap and the Partial Density of states (PDOS) gives information about the origin of bands. In all these self-consistent fields (SCF) calculations, we have used the convergence criteria as the difference between energy in the order of 10^6 Rydberg.

In this chapter, we discuss about:

- Calculation of lattice parameter.
- Calculation of Density of states (DOS) as well as Partial Density of States (PDOS) and plotting.

Then we have performed the series of following convergence tests and energy minimization:

5.2 Structural Optimization:

We carried out the self- consistent field (scf) calculations to determine basic parameters:

kinetic energy cut-off for the plane wave basis and k-points grid by testing the convergence of total energy with these parameters individually and calculation of lattice parameter by energy minimization.

5.2.1 Kinetic Energy cut-off (ecutwfc)

The plane wave scf code implemented in the Quantum Espresso expand the electron wave-function in terms of the infinite basis function that are plane waves. The value of the kinetic energy cut-off corresponds to the neighbouring interactions in the periodic system. If we take this cut-off energy large, we include long range interactions and the results will be more accurate, but this takes more computing resources. If we take this energy small, the results could be inaccurate though computationally cheap. Therefore, we have to take optimum value of this cut-off energy. It is expressed in unit of the energy Ry. The plane wave expansion in the reciprocal space is

$$\psi_k(r) = \frac{1}{\Omega}\sum_G \quad C_{k.G}e^{i(k+G).r} \tag{5.1}$$

where Ω is the volume of the box, G are the reciprocal lattice vectors defined by $G.l = 2\pi m$ for all l, where l is a lattice vector of the crystal and m is an integer, $C_{k.G}$ are the coefficients for the plane waves and k represent the reciprocal space vectors within the first Brillouin zone of the periodic cell.

In principle, we need infinite numbers of plane waves but in order to reduce the computational cost we have to truncate the plane wave expansion from some acceptable value. To make the plane wave expansion (4.1) finite, we truncated according to the condition.

$$\frac{|k+G|^2}{2m} \leq E_{cut} \tag{5.2}$$

We performed the scf calculations using the experimental value of the lattice parameter (a=10.46 Bohr) and some arbitrary k-point mesh in the scf input file for Ca. The scf calculations were performed for different values of the ecutwfc ranging from 40 Ry to 100 Ry. At these different

values of cut-off energy, we found different values of total scf energy. Then we plot the graph between the scf total energy versus kinetic energy cut-off value and the appropriate value of kinetic energy cut-off is chosen from which the convergence of total energy starts to occur. In the case of Calcium, it is found to be 90 Ry, which is shown in the Fig. (5.1). So, for further calculations, the value of ecutwfc = 90 Ry is appropriate to use for Calcium. In our case, the pseudopotential used is PredewBerke-Erzndof (PBE) pseud o-potentials generated using "atomic" code by A. Dal Corso (espresso distribution).

When a graph was plotted for the relationship between cut-off energy along X-axis versus total energy along Y-axis of Ca, following graph was obtained.

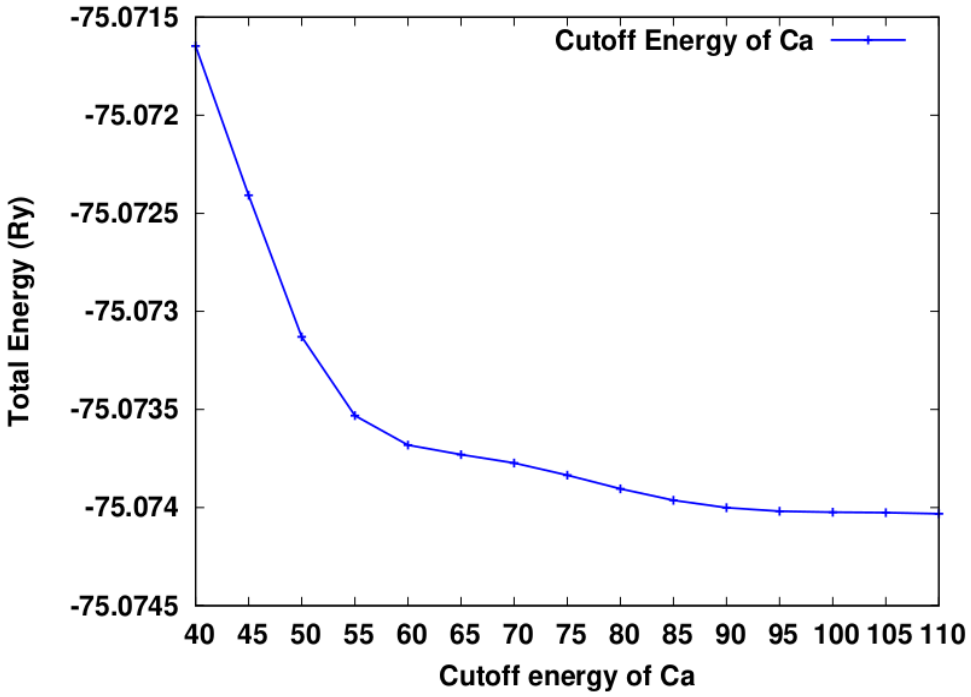

Figure 5.1: The plot of Total energy with cut-off energy of Ca

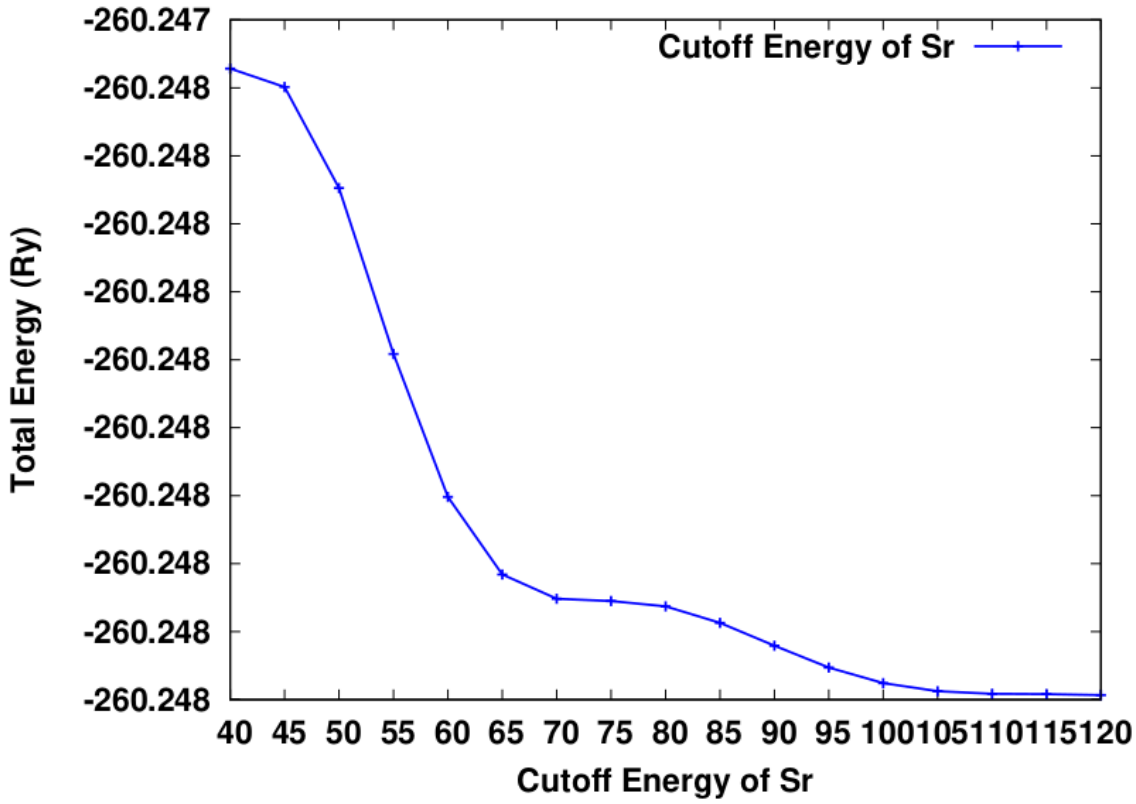

Figure 5.2: The plot of Total energy with cut-off energy of Sr

To determine the value of kinetic energy cut-off we performed the scf calculation using lattice parameter a=11.39 from literature and some arbitrary k-point mess (8, 8, 8) in scf input file for Sr. Similarly we perform same ecutwfc range as Sr in this case and we get different values of total energy in self-consistent field. Then plot of total energy versus kinetic energy cut-off value for FCC structure of Sr is shown in Figure (5.2). Clear from the Fig. (5.2) that there is nominal variation in total energy above 110 Ry. Therefore in the rest of calculations, our cut-off energy is 110 Ry.

5.2.2 Lattice Parameter

Lattice constant is a property of crystal lattice i.e. periodic arrangement of atoms in three dimensions whether it is not a property of atoms. Basically, the lattice constant is the length of periodicity of the lattice repeats itself, for most crystals the lattice constant are few angstroms. After the calculation and value of ecutwfc and, we performed a convergence test for lattice parameter by using the converged value of ecutwfc for both Ca and Sr. For Ca, we performed the scf calculations for total scf energy with different value of lattice parameters ranging from 9.96 to 10.96 Bohrs to optimizing lattice parameter by using optimized value of ecutwfc. Then we plot a graph between total energy with lattice parameter which is shown in Fig. 5.3

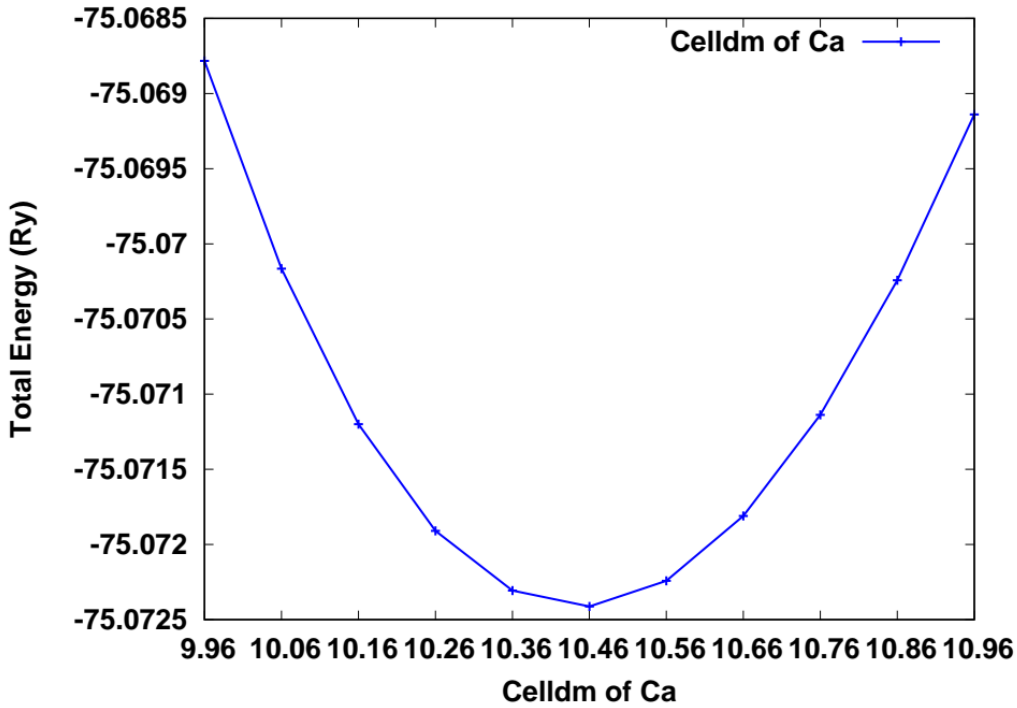

Figure 5.3: The plot of Total energy with lattice parameter of Ca

At different value of lattice parameter we found different value of total energy. Then, we obtained the suitable value of parameters for the input file at which the total energy is minimum. From Fig. 5.3, the appropriate value of lattice parameter is at which the minimum total energy is at 10.46 Bohr. The experimental value of lattice parameter is10.56 Bohr which is closer to our calculate value of lattice parameter and we get 0.95%error from previous work [27].

Then we plot a graph between total energy with lattice parameter which is shown in Fig. 5.4

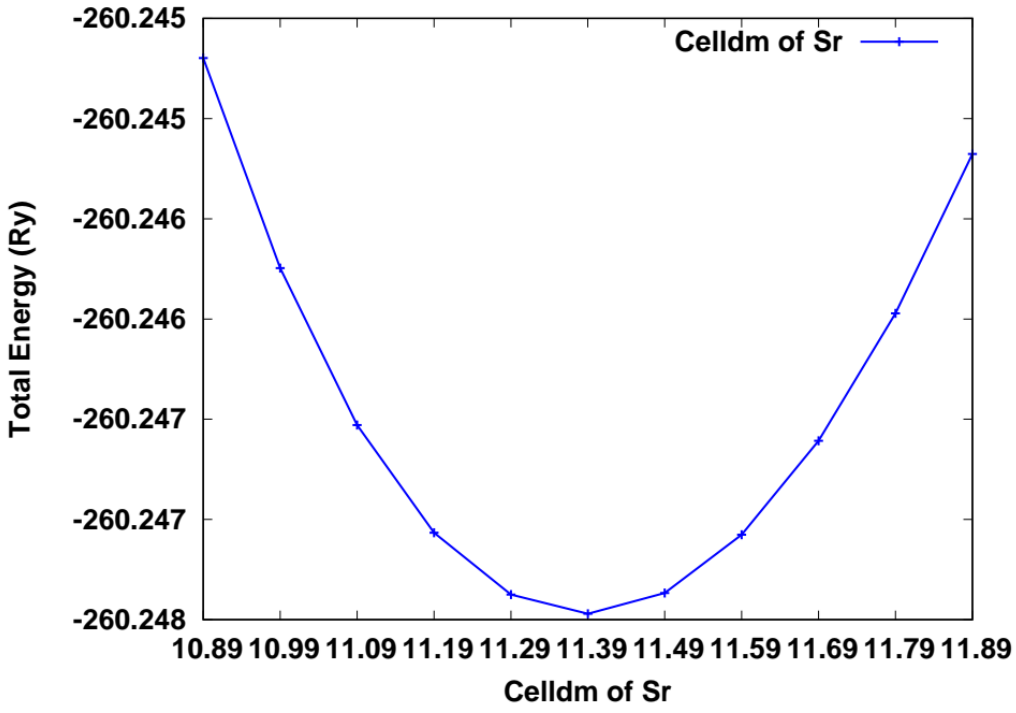

Figure 5.4: The plot of Total energy with lattice parameter of Sr

5.2.3 K-point grid

In order to perform the Brillouin zone interaction in discrete scheme, it is essential to have a large number of grid points. But in practice, due to limitations of computational resources, we optimize the number of k-points grids. By calculating total energy versus k-point grids the rectangular grid of points of dimensions Kx×Ky×Kz, spaced evenly throughout the Brillouin zone is called k-points grid. More the number of the grid points sampling will be more finer and accurate but computationally expensive. Here, the size of grid required depends on the system under study. We can estimate appropriate size by means of total energy calculation. Our approach of k-point sampling is as suggested by Monkhrost and Pack [26]. At first, we performed the scf calculations of Ca for total scf energy with different values of k-points grid starting from 2×2×2 to 20×20×20. The calculated data of k-point grid vs its corresponding total scf energy is shown in Fig. 5.5

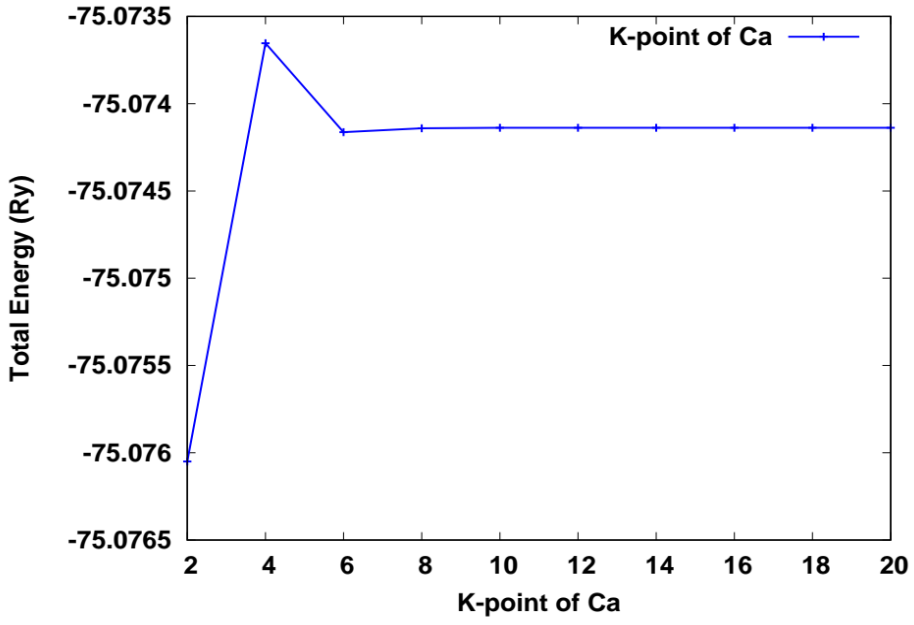

Figure5.5: The plot of Total energy with k-point grid of Ca

From Fig. 5.5 it is clearly seen that total energy of Ca remains almost constant from the k-point grid 6×6×6. So, it is appropriate to use the value of k-point grid as 6×6×6 for our further calculation. Then we performed the scf calculations of Sr for total scf energy with different values of k-points grid starting from 2×2×2 to 18×18×18. The calculated data of k-point grid vs its corresponding total scf energy is shown in Fig.5.6.

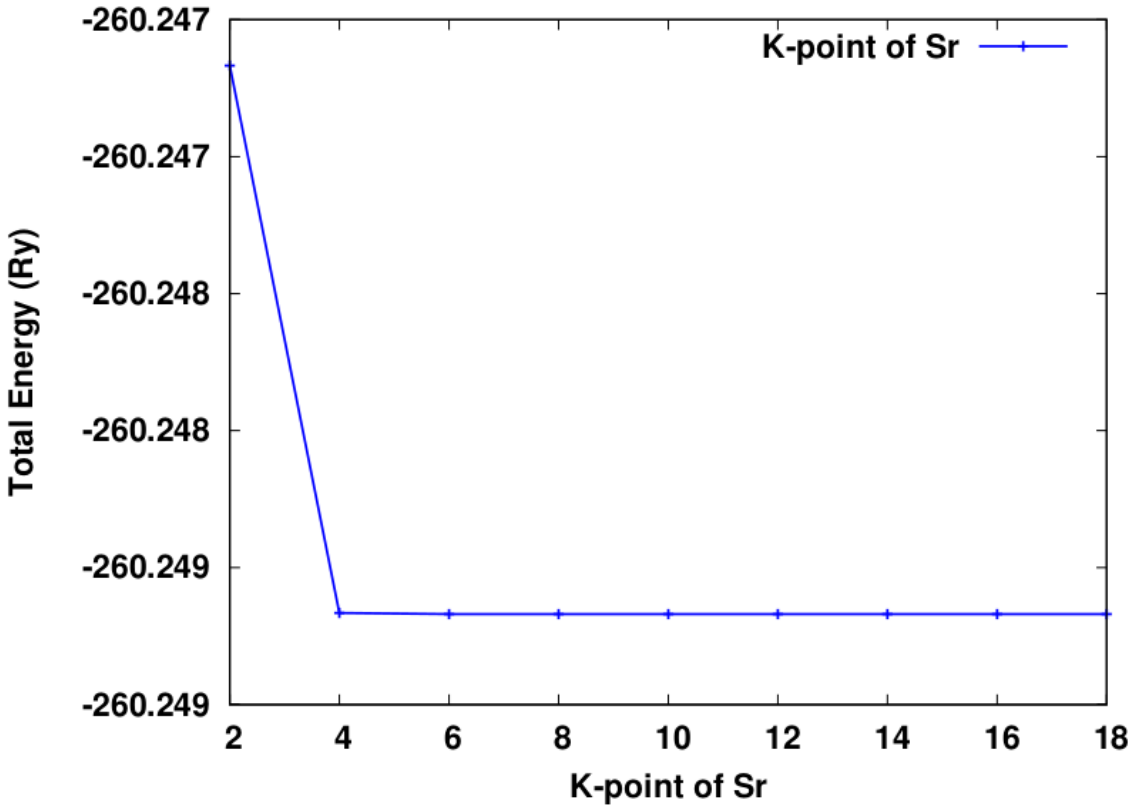

Figure5.6: The plot Total energy with k-point grid of Sr

From Fig. 5.6, it is clearly seen that total energy remains almost constant from the k-point grid4×4×4. So, it is appropriate to use the value of k-point grid as 4×4×4 for our further calculation.

5.2.4 Degauss

In the case of degauss, we should use the smallest value at which our calculation does not struggle to converge. After optimization of all Structure of Ca and Sr, we are intended to study the effect of degauss on elements. To account the degauss, we have taken all optimized value and apply degauss in the range of 0.01 to 0.1. Then we plotted a graph between degauss value vs total kinetic energy which is shown in Figure 5.7 and figure 4.8 for Ca and Sr respectively. From the graph it is observed that degauss is is minimum at 0.03 so further calculation take place by using degauss 0.03. Also, from graph 4.8 the minimum value is at 0.1 so we took 0.1 for further calculations of Sr.

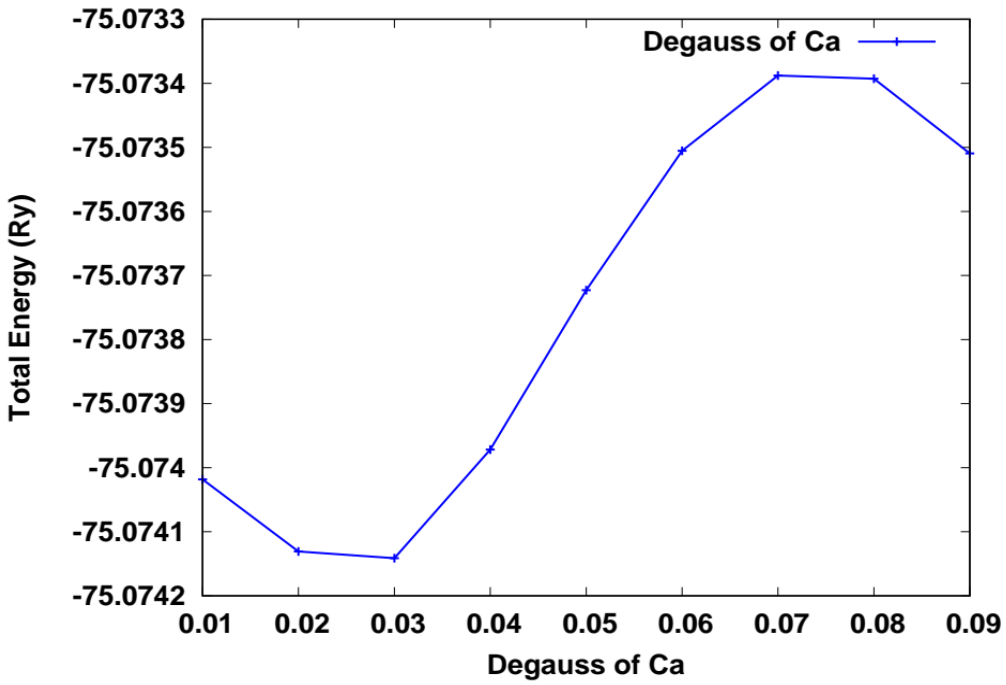

Figure 5.7: The plot of Total energy with degauss of Ca

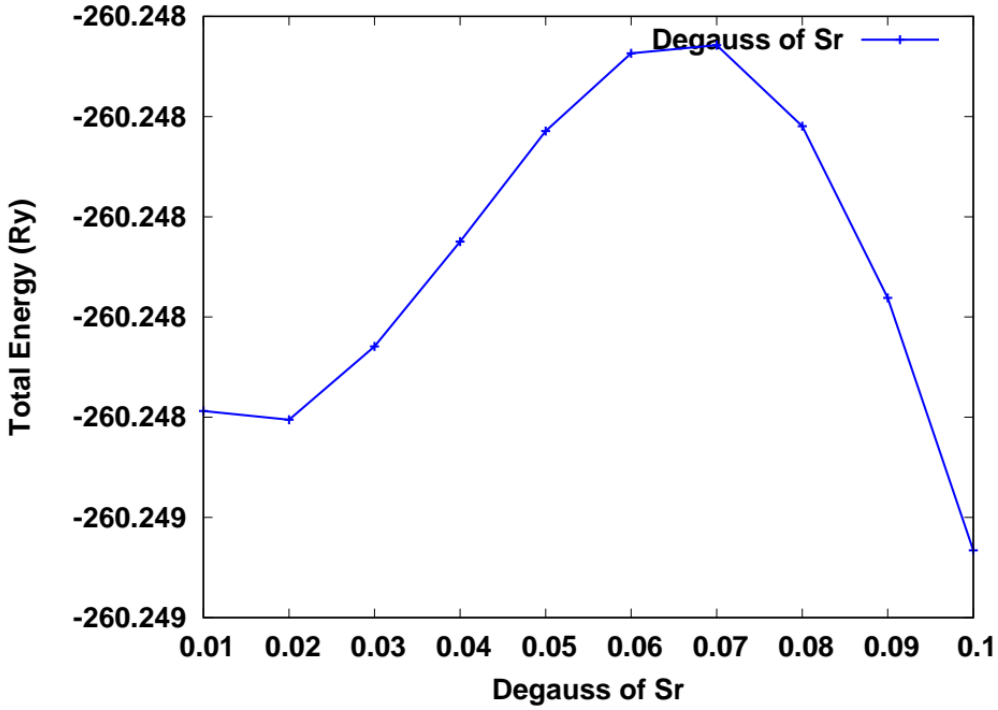

Figure 5.8: The plot of Total energy with degauss of Sr

We have also calculated the band structure of Transition Metal Ca and Sr. For other calculations of Ca and Sr, we took (6×6×6) and (4×4×4) respectively k-points along specific direction of irreducible Brillouin zone in order to obtain fine band structure which is performed by executable pw.x. Then, we performed post processing calculations with executable plotband.x in order to obtain band structure of Calcium (Ca) and Strontium (Sr). Further, we have calculated the DOS and PDOS for both Ca and Sr structure. Finally we performed scf calculation and then nscf calculation; we used denser k-point mesh in order to obtain smooth partial density of states curve. These calculations were performed using the executable pw.x. Then, we performed PDOS calculation using executables projwfc.x command. In this section, we discussed the results of the first principles calculations carried out to obtain: Band structure calculation of Ca and Sr, Density of states of structure of Ca and Sr and Partial Density of states of structure of Ca and Sr

5.3 Band Structure

In the first principles electronic structure calculation of crystals, the electronic band structure is one of the most widely applied analytical tools especially within the Kohnsham framework of density functional theory. The band structures of solid are helpful to determine different electronic properties of solid. It contains the basic ingredients to almost all the crystal properties. Since the atoms in a solid are closely packed the interaction between them perturbed the initial atomic levels when a large number of atoms are brought together. Electrons in the orbitals are filled up according to Pauli's exclusion principle i.e. no two electrons can occupy the same energy state. A bands constitutes a sort of energy continuum, in which separate level due to individual atoms cannot be identified. In the process of inter atomic interaction, the inner shell electron stated are the least affected. Whereas the valance electron, which are closest to neighbouring ions, are the most affected. The effect of bringing one atom closer to the other is to split a single sharp level. The bands structures of solids are helpful in determining different electronic and optical properties of the solid.

The band structure is calculated by pseudo potential and plane wave basis set method within the Density functional theory (DFT), treating exchange- correlation functional with generalized gradient approximation (GGA) in the form of PredewBerke- Erzndof (PBE) functional. All pseudo potential used in the calculations were norm- conserving scalar relativistic and full relativistic pseudo potentials. All calculation was performed within the Quantum- ESPRESSO package, plane wave kinetic energy cut-off were set at 90 Ry for Ca and 110 Ry for Sr. We took uniform grid of k-vector (k-points) in X-Y plane ranging from 1 to 1 in the unit of 2π a .

The band structure calculation of Ca is shown in Fig. 5.9. From graph the calculated value of band gap is found to be nearly 0ev. Valence band and Conduction band touch at G (k-path) which is found quite similar to previous result.

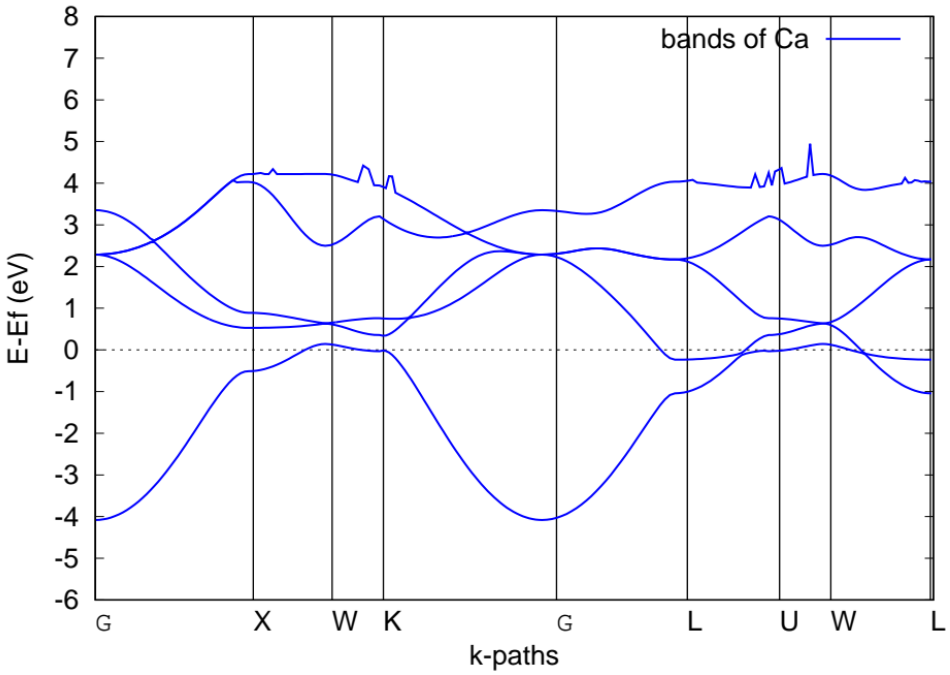

Figure5.9: the plot of energy gap between conduction and valence band of Ca

The band structure calculation of Sr is shown in Fig. 5.10. From figure it is found that the value of band gap is almost 0ev because of the overlap at G (k-path). Our work result is closely same as previous worker result.

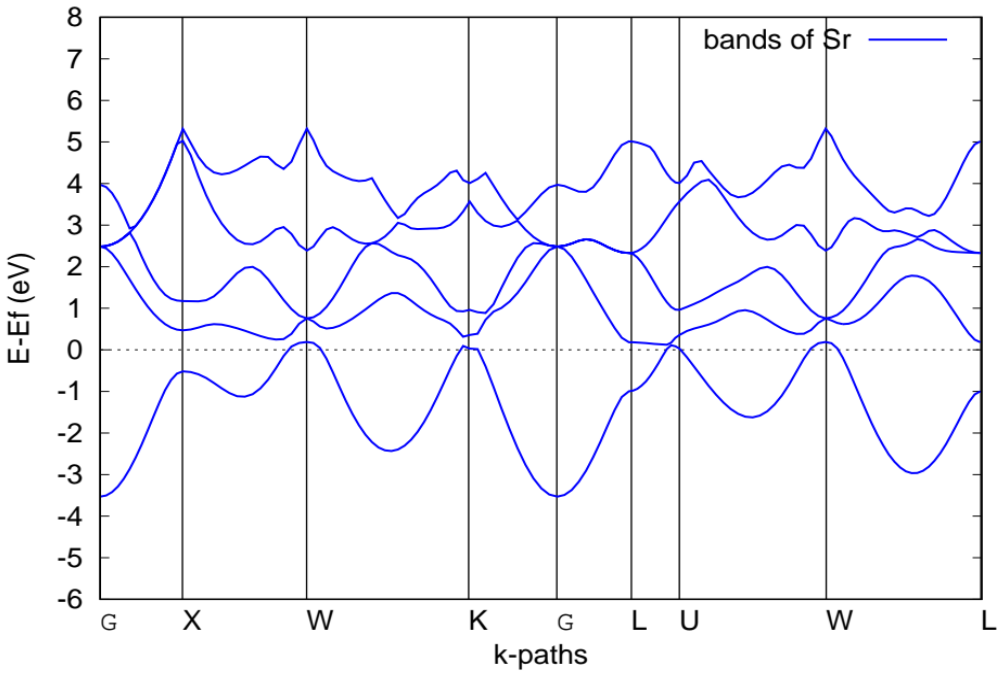

Figure5.10: The plot of energy gap between conduction and valence band of Sr

5.4 Density of States

The density of states (DOS) is defined as the number of states per unit energy range available for the particles to be occupied. In other words, the density of states refers to the number of quantum states per unit energy range and it indicates how density packed quantum states in a particular system. In solid state and condense matter physics, the density of states is of immense important as it can be used to calculate the various parameters that give the insight of the different electronic, magnetic and transport properties. For example, Specific heat and paramagnetic susceptibility of a substance, mobility of charge carriers, diffusion properties and so on can be readily computed with the knowledges of density of states (DOS). Moreover, the density of states provides numerical information on the states that are available at each energy level. The value of zero density of states indicates that there are no available states for occupation in an energetic level

The density of sates is calculated by pseudopotential and plane wave basis set method within the Density functional theory (DFT), treating exchange- correlation functional with generalized gradient approximation (GGA) in the form of PredewBerke- Erzndof (PBE) functional. All pseudopotential used in the calculations were norm- conserving scalar relativistic and full relativistic pseudopotentials. All calculation was performed within the Quantum- Espresso package, plane wave kinetic energy cut-off was set at 90 Ry for Ca and 110 Ry for Sr.

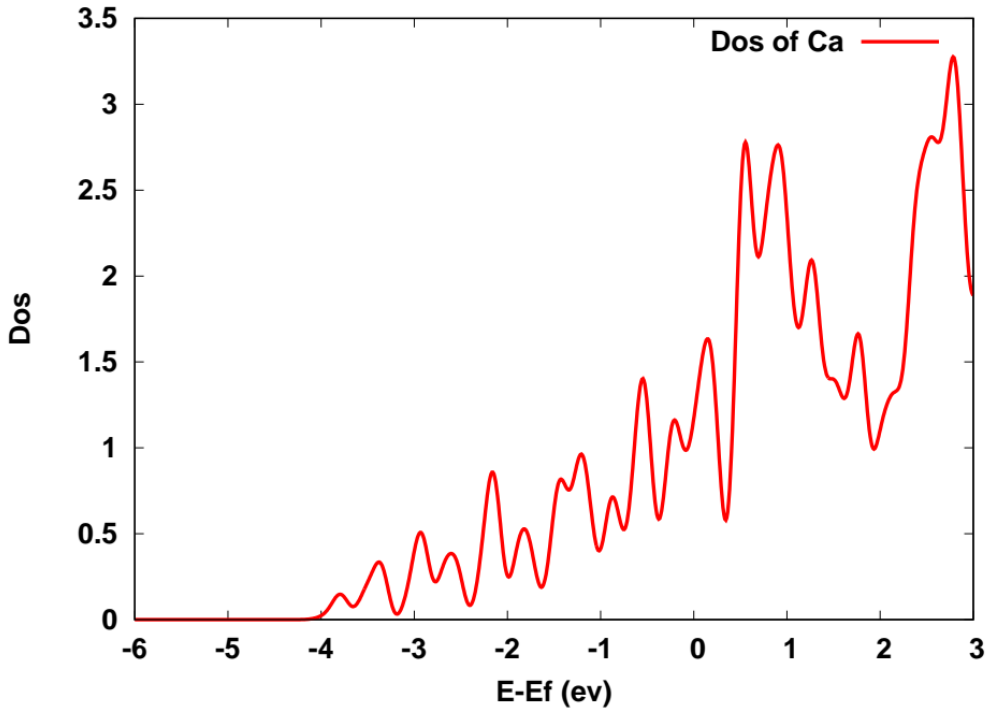

Figure5.13: DOS curve of Ca with energies at DeltE=0.01

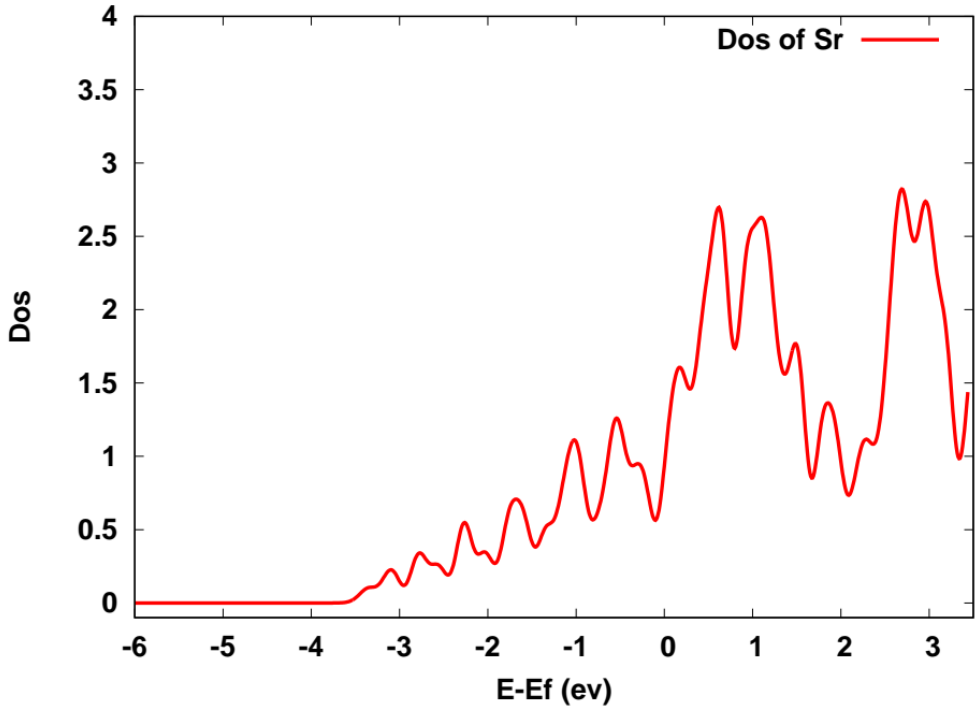

Figure5.14: DOS curve of Sr with energies at DeltE=0.01

The results of density of Ca and Sr help to further elaborate the nature of the band gap as shown in above Fig. 5.11 and Fig. 5.12, Where density of states DeltE=0.01, shows the respective states of crystal which clarify the nature of the element. For the comparative study of the band structures and density of states, we have merge the figure of band structures and density of states of Alkaline Earth metal of Ca and Sr in suitable scale which is shown in Fig.5.13 and Fig.5.14 respectively.

5.5 Partial Density of States

The results of partial densities of states (PDOS) of Ca and Sr help to further elaborate the nature of band gap as shown in Fig. 5.15 and Fig.5.16. The partial density of states gives information about the origin of bands.

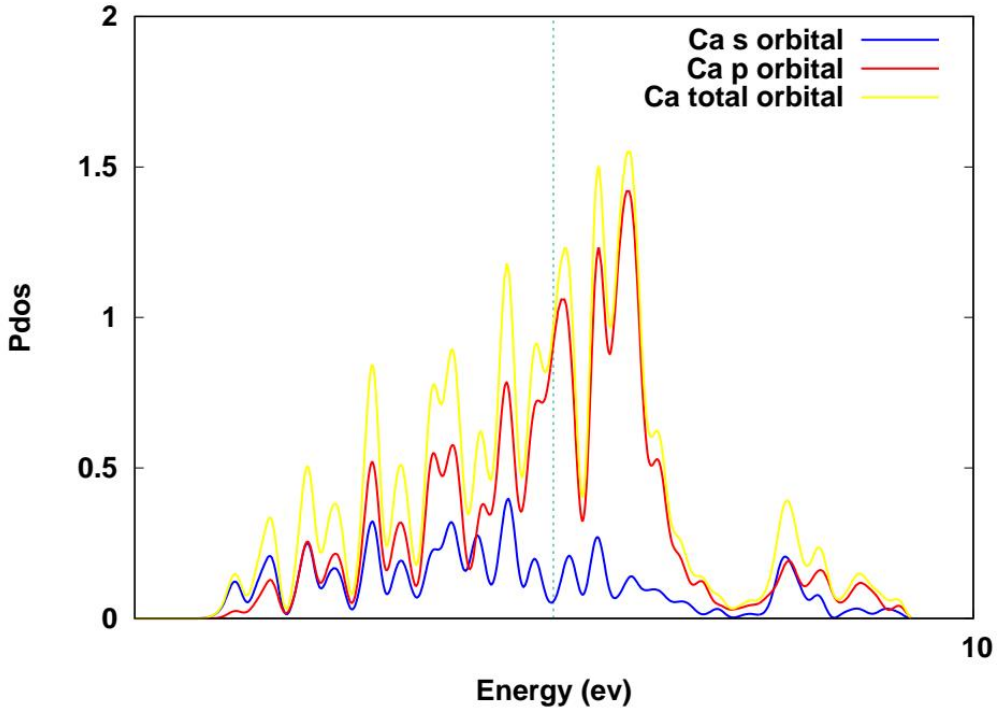

Figure5.15: PDOS curve of Ca with energies at DeltE=0.01

CHAPTER 6

CONCLUSION AND CONCLUDING REMARKS:

This thesis has successfully employed to examine the structural properties of Alkaline earth element Ca and Sr with the help of DFT, GGA, implemented with Quantum ESPRESSO code. At first we have constructed optimized structure of unit cell of FCC structure of both Ca and Sr. During optimization, the kinetic energy cut-off energy is found to be 90 Ry having k-point grid $6 \times 6 \times 6$ for Ca. Then we estimate the lattice Parameter is found to be 10.46 Bohr for Ca which is very near with experimental results as well as previous calculated data. Which is only 0.95% deviated from experimental result and previous data. Thus the lattice parameter of Ca estimated with GGA method is in close agreement with experimental values. Then we have study the band structure, density of states and partial density of states of Ca using GGA method in QE package.

Similarly, optimization, the kinetic energy cut-off energy is found to be 110 Ry having k-point grid $4 \times 4 \times 4$ for Sr. Then we estimate the lattice Parameter is found to be 11.49 Bohr for Sr which is very near with experimental results as well as previous calculated data. Which is only 0.9% deviated from experimental result and previous data. Thus the lattice parameter of Sr estimated with GGA method is in close agreement with experimental values. Then we have study the band structure, density of states and partial density of states of Ca using GGA method in QE package.

This shows that Quantum ESPRESSO code using the plane-wave pseudopotential method can be used to perform first-principles calculations to study the electronic and other system which is more complex of active metals. We belive code can be used to study correlated systems for interest to current research to amble technological potential they support. All our study method which we have performs in this work can be used standard frame work to calculate the

electronic, magnetic, and structural properties of materials in the elements and other related materials for which experimental data are not available.

6.1 Further Enhancement

The following studies can be done as further enhancement in our present study.

- Similar study from metal at least few more candidates, possibly adding optical and phonon properties can be done in future.
- We also can study the effect of doping of other suitable atom, which would give rise to alloy of different properties.
- We can also study same from other different method suitable for these elements.

Thus we are now willing to extend our work to study the magnetic properties and phonon calculation, thermal expansion, optical properties which may have many potential applications in modern electronics.

BIBLIOGRAPHY

[1] Robert H. Crabtree, *The Organometallic Chemistry of the Transition Metals* John Wiley & Sons, Inc., Hoboken, New Jersey (2014)

[2] J. R. Hook, H. E. Hall, *Solid state physics*, Wiley (1991)

[3] Harald Ibach, Hans L., *Solid-state physics an introduction to Principle of material science*, Springer Verlag Berlin Heidelberg, (2009)

[4] pinterest.com Retrieved 20 August 2020

[5] slideplayer.com Retrieved 20 August 2020

[6] Richard J. D. Tilley - *Crystals and Crystal Structures*, Wiley (2006)

[7] wikipedia.org Retrieved 20 August 2020

[8] iopscience.iop.org Retrieved 20 August 2020

[9] slideshare.net Retrieved 20 August 2020

[10] Giuseppe Iadonisi, Giovanni Cantele, Maria Luisa Chiofalo, *Introduction to Solid State Physics and Crystalline Nanostructures*, Springer-Verlag Mailand, (2014)

[11] R.Murugeshan *Modern Physics* S. Chand, New Delhi (2009)

[12] Charles Kittel *Introduction to Solid State Physics*, Wiley (2005)

[13] en.wikipedia.org Retrieved 20 August 2020

[14] en.wikipedia.org Retrived 20 August 2020

[15] e-education.psu.edu Retrived 20 August 2020

[16] J W Mullin *Crystallization*, Butterworth-Heinemann (2001)

[17] Ashcroft, Neil W, Mermin, David N - *Solid State Physics(2006)*

[18] en.wikipedia.org Retrived 10 june 2020

[19] Vishnu Swarup Mathur, Surendra Singh - *Concepts in Quantum Mechanics*-Chapman &Hall_CRC (2009)

[20] C. R. Hammond *The elements* (p. 4–35) in *Lide, D. R., ed. (2005). CRC Handbook of Chemistry and Physics (86th ed.). Boca Raton (FL): CRC Press*

[21] Berner, Robert (2003). "The long-term carbon cycle, fossil fuels and atmospheric composition". *Nature*. **426** (6964): 323–326

[22] Zeebe (2006). "Marine carbonate chemistry". National Council for Science and the Environment. Retrieved 2010-03-13

[23] C. R. Hammond *The elements* (pp. 4–35) in *Lide, D. R., ed. (2005). CRC Handbook of Chemistry and Physics (86th ed.). Boca Raton (FL): CRC Press*

[24] Greenwood and Earnshaw, p. 19

[25] MacMillan, J. Paul; Park, Jai Won; Gerstenberg, Rolf; Wagner, Heinz; Köhler, Karl and Wallbrecht, Peter (2002) "Strontium and Strontium Compounds" in *Ullmann's Encyclopedia of Industrial Chemistry*, Wiley-VCH, Weinheim.

[26] ICF Incorporated, USEP Agency. Archived from the original (PDF) on 19 December 2008. Retrieved 7 January 2012.

[27] Ober, Joyce A.; Polyak, Désirée E. "Mineral Yearbook 2007: Strontium" (PDF). United States Geological Survey. Retrieved 14 October 2008.

[28] Barnett-Johnson, Rachel; Grimes, Churchill B.; Royer, Chantell F.; Donohoe, Christopher J. (2007). "Identifying the contribution of wild and hatchery Chinook salmon (Oncorhynchus tshawytscha) to the ocean fishery using otolith microstructure as natural tags". *Canadian Journal of Fisheries and Aquatic Sciences*.

[29] Porder, S.; Paytan, A. & E.A. Hadly (2003). "Mapping the origin of faunal assemblages using strontium isotopes". *Paleobiology*. **29** (2): 197–204

[30] Ghom (1 December 2005). *Textbook of Oral Medicine*. p. 885.

[31] Meunier P. J.; Roux C.; Seeman E.; Ortolani, S.; Badurski, J. E.; Spector, T. D.; Cannata, J.; Balogh, A.; Lemmel, E. M.; Pors-Nielsen, S.; Rizzoli, R.; Genant, H. K.; Reginster, J. Y. (January 2004)

[32] Reginster JY; Seeman E; De Vernejoul MC; Adami, S.; Compston, J.; Phenekos, C.; Devogelaer, J. P.; Diaz Curiel, M.; Sawicki, A.; Goemaere, S.; Sorensen, O. H.; Felsenberg, D.; Meunier, P. J. (May 2005)

[33] Medicines and Healthcare products Regulatory Agency, UK. March 2014.

[34] Price, Charles T.; Langford, Joshua R.; Liporace, Frank A. (5 April 2012).

[35] "Strontium". *WebMD*. Retrieved 20 August 2020.

[36] "Strontium for Osteoporosis". WebMD. Retrieved 20 August 2020.

[37] P. Blaha and J callaway phy. Rev. B32 (December 1985)

[38] M Tegze and J Hafner vol.1 p. 8277(1989)

[35] Journal of physics F Metal physics vol.1 S.chatterjee & D.K Chakraborti (2000)

[36] Julia F.Medveda Emily N. Teasley Michael Hoffman Phy Rev. B76 (9 oct. 2007)

[37] Wiley-vch Verlag Gmbh & Co. Weinheim (2004)

[38] V.M Zainullinar, M.A Korotin & V.L Kozhevnikov The European physical Journal B – considered Matter and Complex System page 425 (2006)

APPENDIX

[A]. LIST OF TABLES:

Table 1: Table of cut-off kinetic energy and its corresponding total energy of Ca:

cut-off energy (Ry)	Total energy (Ry)
40	-75.07164705
45	-75.07240840
50	-75.07312998
55	-75.07353119
60	-75.07368131
65	-75.07373008
70	-75.07383472
75	-75.07383472
80	-75.07390380
85	-75.07396242
90	-75.07400039
95	-75.07401815
100	-75.07402360
105	-75.07402569
110	-75.07403103

Table 2: Table of cut-off kinetic energy and its corresponding total energy of Sr

cut-off energy (Ry)	Total energy (Ry
40	-260.24747178
45	-260.24749888
50	-260.24764746
55	-260.24789148
60	-260.24810183
65	-260.24821602
70	-260.24825167
75	-260.24825488
80	-260.24826278
85	-260.24828711
90	-260.24832072
95	-260.24835281
100	-260.24837582
105	-260.24838773
110	-260.24839141
115	-260.24839187
120	-260.24839332

Table 3: The Variation of total energy with k-point grid of Ca

K-point	Total energy (Ry)
2	-75.07604969
4	-75.07365379
6	-75.07416270
8	-75.07414118
10	-75.07413772
12	-75.07413805
14	-75.07413806
16	-75.07413808
18	-75.07413808
20	-75.07413807

Table 4: The Variation of total energy with k-point grid of Sr:

K-point	Total energy (Ry)
2	-260.24666763
4	-260.24866559
6	-260.24866949
8	-260.24866940
10	-260.24866939
12	-260.24866939
14	-260.24866939
16	-260.24866939
18	-260.24866939

Table 5: The Variation of total energy with lattice constant of Ca:

Lattice constant (Bohr)	Total energy (Ry)
9.96	-75.06878245
10.06	-75.07016535
10.16	-75.07119978
10.26	-75.07190977
10.36	-75.07230619
10.46	-75.07241252
10.56	-75.07224217
10.66	-75.07181009
10.76	-75.07113815
10.86	-75.07024196
10.96	-75.06913903

Table 6: The Variation of total energy with lattice constant of Sr:

Lattice constant (Bohr)	Total energy (Ry)
5.408	-5.83984760
5.508	-5.84697086
5.608	-5.85199946
5.708	-5.85481642
5.808	-5.85663368
5.908	-5.85762060
6.008	-5.85774556
6.066	-5.85745096
6.108	-5.85708141
6.208	-5.85564528
6.308	-5.85329330
6.408	-5.84984608
6.508	-5.84520775
6.608	-5.83943438

Table 7: The Variation of total energy with degauss of Ca:

degauss	Total energy (Ry)
0.01	-75.07401815
0.02	-75.07413077
0.03	-75.07414118
0.04	-75.07397174
0.05	-75.07372279
0.06	-75.07350542
0.07	-75.07338782
0.08	-75.07339285
0.09	-75.07350930

Table 8: The Variation of total energy with degauss of Sr:

degauss	Total energy (Ry)
0.01	-260.24838773
0.02	-260.24840503
0.03	-260.24825868
0.04	-260.24804956
0.05	-260.24782887
0.06	-260.24767384
0.07	-260.24765754
0.08	-260.24781919
0.09	-260.24816183
0.10	-260.24866573

[B]. Different input Files:

List 1: Input script for scf final

Ca

```
&control
calculation='scf',
restart_mode='from_scratch',
pseudo_dir ='/home/abc/qe-6.5/pseudo',
outdir='./',
prefix='Ca',
/
&system
ibrav=2
celldm(1)=10.46
nat=1
ntyp=1
ecutwfc=90.0
ecutrho=720.0
occupations='smearing'
smearing='mp'
degauss=0.03
/
&electrons
conv_thr = 1.0e-10
mixing_beta = 0.7
/
```

ATOMIC_SPECIES

Ca 40.078 Ca.pbe-spn-rrkjus_psl.1.0.0.UPF

ATOMIC_POSITIONS {alat}

Ca 0.00 0.00 0.00

K_POINTS {automatic}

6 6 6 1 1 1

Sr

&control

calculation='scf',

restart_mode='from_scratch',

pseudo_dir ='/home/abc/qe-6.5/pseudo',

outdir='./',

prefix='Sr',

/

&system

ibrav=2

celldm(1)=11.39

nat=1

ntyp=1

ecutwfc=110

ecutrho=880

occupations='smearing'

smearing='mp'

degauss=0.10

/

```
&electrons
conv_thr = 1.0e-10
mixing_beta = 0.7
/
ATOMIC_SPECIES
Sr 87.62 Sr.pbe-spn-kjpaw_psl.1.0.0.UPF
ATOMIC_POSITIONS {alat}
Sr 0.00 0.00 0.00
K_POINTS {automatic}
4 4 4 1 1 1
```

List 2: Input script for nscf calculation of Band

Ca

```
&control
calculation='nscf',
restart_mode='from_scratch',
pseudo_dir ='/home/abc/qe-6.5/pseudo',
outdir='./',
prefix='Ca',
/
&system
ibrav=2
celldm(1)=10.46
nat=1
ntyp=1
ecutwfc=90.0
```

ecutrho=900.0

occupations='smearing'

smearing='mp'

degauss=0.03

/

&electrons

conv_thr = 1.0e-10

mixing_beta = 0.7

/

ATOMIC_SPECIES

Ca 40.078 Ca.pbe-spn-rrkjus_psl.1.0.0.UPF

ATOMIC_POSITIONS {alat}

Ca 0.00 0.00 0.00

K_POINTS {automatic}

10 10 10 0 0 0

Sr

&control

calculation='nscf',

restart_mode='from_scratch',

pseudo_dir ='/home/abc/qe-6.5/pseudo',

outdir='./',

prefix='Sr',

/

&system

ibrav=2

celldm(1)=11.39

nat=1

ntyp=1

ecutwfc=110

ecutrho=880

occupations='smearing'

smearing='mp'

degauss=0.01

/

&electrons

conv_thr = 1.0e-10

mixing_beta = 0.7

/

ATOMIC_SPECIES

Sr 87.62 Sr.pbe-spn-kjpaw_psl.1.0.0.UPF

ATOMIC_POSITIONS {alat}

Sr 0.00 0.00 0.00

K_POINTS {automatic}

12 12 12 0 0 0

List 3: Input script for Band.in

Ca

&control

calculation='scf',

restart_mode='from_scratch',

```
pseudo_dir ='/home/abc/qe-6.5/pseudo',
outdir='./',
prefix='Ca',
/
&system
ibrav=2
celldm(1)=10.46
nat=1
ntyp=1
ecutwfc=90.0
ecutrho=720.0
occupations='smearing'
smearing='mp'
degauss=0.02
/
&electrons
conv_thr = 1.0e-10
mixing_beta = 0.7
/
ATOMIC_SPECIES
Ca 40.078 Ca.pbe-spn-rrkjus_psl.1.0.0.UPF
ATOMIC_POSITIONS {alat}
Ca 0.00 0.00 0.00
K_POINTS {crystal_b}
9
```

0.000 0.000 0.000 39 G

-0.500 -0.500 0.000 19 X

-0.750 -0.500 -0.250 10 W

-0.750 -0.375 -0.375 51 K

0.000 0.000 0.000 27 G

-0.500 0.000 0.000 21 L

-0.625 -0.375 0.000 17 U

-0.750 -0.500 -0.250 33 W

-0.500 0.000 0.000 39 L.

/

Sr

&control

calculation='bands',

restart_mode='from_scratch',

pseudo_dir ='/home/abc/qe-6.5/pseudo',

outdir='./',

prefix='Sr',

/

&system

ibrav=2

celldm(1)=11.39

nat=1

ntyp=1

ecutwfc=110

ecutrho=880

```
occupations='smearing'
smearing='mp'
degauss=0.10
/
&electrons
conv_thr = 1.0e-10
mixing_beta = 0.7
/
ATOMIC_SPECIES
Sr 87.62 Sr.pbe-spn-kjpaw_psl.1.0.0.UPF
ATOMIC_POSITIONS {alat}
Sr 0.00 0.00 0.00
K_POINTS {crystal_b}
9
      0.000    0.000    0.000   14  G
         0.000   -0.500   -0.500   16  X
     -0.750   -0.250   -0.500   25  W
      0.375   -0.375    0.000   11  K
      0.000    0.000    0.000   10  G
      0.500    0.000    0.000   12  L
      0.250   -0.375   -0.375   20  U
     -0.750   -0.250   -0.500   27  W
      0.500    0.000    0.000   14  L
```

List:4 Input Script For Bands.in

Ca

&bands

prefix = 'Ca'

outdir = './'

filband = 'Ca.bands.dat'

lsym = .true.,

/

Sr

&bands

prefix = 'Sr'

outdir = './'

filband = 'Sr.bands.dat'

lsym = .true.,

/

List:5 Input Script For Dos

Ca

&dos

prefix='Ca'

outdir='./'

ngauss=-1

degauss=0.01

DeltaE=0.01

fildos='Ca.dos.dat'

/

Sr

```
&dos
prefix='Sr'
outdir='./'
ngauss=-1
degauss=0.01
DeltaE=0.01
fildos='Sr.dos.dat'
/
```

List 6: Input script for PDOS.in

Ca

```
&projwfc
   prefix='Ca'
   outdir='./'
   ngauss=-1
   degauss=0.01
   DeltaE=0.01
   filpdos='Ca.pdos.dat'
/
```

Sr

```
&projwfc
   prefix='Sr'
   outdir='./'
   ngauss=-1
```

```
   degauss=0.03
   DeltaE=0.01
   filpdos='Sr.pdos.dat'
/
```

List 7: Input script for Scf Plot

Ca

```
set term postscript enhanced color 'Helvetica-Bold'20
set output 'Ca.k-point.ps'
set autoscale
unset log
unset label
set xtic 2,2
#set ytic 2,0.2
set xlabel "K-point of Ca"
set ylabel "Total Energy (Ry)"
set xr [2:20]

plot "Ca.k-point.dat" using 1:2 title 'K-point of Ca' w lp lw 3 lt 1 lc rgb "blue",\

set output
 !ps2pdf Ca.k-point.ps
 !rm Ca.k-point.ps
pause -1 "hit any key to continue\n"
```

Sr

```
set term postscript enhanced color 'Helvetica-Bold'20
set output 'Sr.k-pont.ps'
set autoscale
unset log
unset label
set xtic 2,2
#set ytic 2,0.2
set xlabel "K-point of Sr"
set ylabel "Total Energy (Ry)"
set xr [2:18]

plot "Sr.k-point.dat" using 1:2 title 'K-point of Sr' w lp lw 3 lt 1 lc rgb "blue",\

set output
 !ps2pdf Sr.k-point.ps
 !rm Sr.k-point.ps
pause -1 "hit any key to continue\n"
```

List 8: Input script for bands plot

Ca

```
set terminal postscript enhanced color "Helvetica" 20
set output "Ca.band.ps"
set autoscale
unset log
set xzeroaxis lw 2 lc -1
```

```
unset xtics
set ytics -15,1
set bmargin 3
set xlabel "k-paths" offset 0,-1,0
set ylabel "E-Ef (eV)"
set label "{/symbol G}" at 0.00000,-6.513
set label "{/symbol G}" at 3.00873,-6.513
set label "X" at 1.03039, -6.513
set label "W" at 1.54437, -6.513
set label "K" at 1.87894, -6.513
set label "L" at 3.86213, -6.513
set label "U" at 4.46339, -6.513
set label "W" at 4.79796, -6.513
set label "L" at 5.44771, -6.513
set arrow from 0.00000, graph 0 to 0.00000, graph 1 nohead
set arrow from 1.03039, graph 0 to 1.03039, graph 1 nohead
set arrow from 1.54437, graph 0 to 1.54437, graph 1 nohead
set arrow from 1.87894, graph 0 to 1.87894, graph 1 nohead
set arrow from 3.00873, graph 0 to 3.00873, graph 1 nohead
set arrow from 3.86213, graph 0 to 3.86213, graph 1 nohead
set arrow from 4.46339, graph 0 to 4.46339, graph 1 nohead
set arrow from 4.79796, graph 0 to 4.79796, graph 1 nohead
set arrow from 5.44771, graph 0 to 5.44771, graph 1 nohead
#set key 0.01,100
set xr [0.0:5.46771]
```

```
set yr [-6:8]
ef=5.0534
plot "Ca.bands.dat.gnu" using 1:($2-ef) title 'bands of Ca' w l lw 3 lt 4 lc rgb "blue"
set output
! ps2pdf Ca.band.ps
! rm Ca.band.ps
pause -1 "Hit any key to continue\n"
```

Sr

```
set terminal postscript enhanced color "Helvetica" 20
set output "Sr.band.ps"
set autoscale
unset log
set xzeroaxis lw 2 lc -1
unset xtics
set ytics -15,1
set bmargin 3
set xlabel "k-paths" offset 0,-1,0
set ylabel "E-Ef (eV)"
set label "{/symbol G}" at 0.00000,-6.513
set label "{/symbol G}" at 5.52287,-6.513
set label "X" at 0.994020, -6.513
set label "W" at 2.49717, -6.513
set label "K" at 4.45602, -6.513
set label "L" at 6.42476, -6.513
set label "U" at 7.00603, -6.513
```

```
set label "W" at 8.78102, -6.513

set label "L" at 10.6520, -6.513

set arrow from 0.00000, graph 0 to 0.00000, graph 1 nohead

set arrow from 0.994020, graph 0 to 0.994020, graph 1 nohead

set arrow from 2.49717, graph 0 to 2.49717, graph 1 nohead

set arrow from 4.45602, graph 0 to 4.45602, graph 1 nohead

set arrow from 5.52287, graph 0 to 5.52287, graph 1 nohead

set arrow from 6.42476, graph 0 to 6.42476, graph 1 nohead

set arrow from 7.00603, graph 0 to 7.00603, graph 1 nohead

set arrow from 8.78102, graph 0 to 8.78102, graph 1 nohead

set arrow from 10.6530, graph 0 to 10.6530, graph 1 nohead

#set key 0.01,100

set xr [0.0:10.6630]

set yr [-6:8]

ef=5.0343

plot "Sr.bands.dat.gnu" using 1:($2-ef) title 'bands of Sr' w l lw 3 lt 4 lc rgb "blue"

set output

! ps2pdf Sr.band.ps

! rm Sr.band.ps

pause -1 "Hit any key to continue\n"
```

List 9: Input script for plot dos

Ca

```
set term postscript enhanced color 'Helvetica-Bold' 20

set output 'Ca.dos.ps'

set autoscale
```

```
unset log

unset label

set xtic -10,1

set ytic 0,0.5

set xlabel "E-Ef (ev)"

set ylabel "Dos"

#set key 0.01,100

set xr [-6:3]

#set yr [0:325]

ef=4.992

plot "Ca.dos.dat" using ($1-ef):2 title 'Dos of Ca'  w l lw 5 lt 5 lc rgb "red"

set output

! ps2pdf Ca.dos.ps

! rm Ca.dos.ps

pause -1 "Hit any key to continue\n"
```

Sr

```
set term postscript enhanced color 'Helvetica-Bold' 20

set output 'Sr.dos.ps'

set autoscale

unset log

unset label

set xtic -10,1

set ytic auto
```

```
set xlabel "E-Ef (ev)"

set ylabel "Dos"

#set key 0.1,10

set xr [-6:3.5]

set yr [-0.1:4]

ef= 5.0343

plot "Sr.dos.dat" using ($1-ef):2 title 'Dos of Sr'  w l lw 5 lt 5 lc rgb "red"

set output

! ps2pdf Sr.dos.ps

! rm Sr.dos.ps

pause -1 "Hit any key to continue\n"
```

List 10: Input Script for Pdos

Ca

```
set term postscript enhanced color 'Helvetica-Bold' 20

set output 'Ca.pdos.ps'

set autoscale

unset log

unset label

set xtic 10,1

set ytic auto

set xlabel "Energy (ev)"

set ylabel "Pdos"
```

```
set xr [0:10]
set yr [0:2]
set arrow from 4.9923,0.0 to 4.9923,2, 2 nohead ls 10 dt 2
plot  "atom_Ca_s.dat" using 1:2 title 'Ca s orbital' w l lw 3 lt 1 lc rgb "blue",\
     "atom_Ca_p.dat" using 1:2 title 'Ca p orbital' w l lw 3 lt 1 lc rgb "red",\
     "atom_Ca_tot.dat" using 1:2 title 'Ca total orbital' w l lw 3 lt 1 lc rgb "yellow",

set output
 ! ps2pdf Ca.pdos.ps
 ! rm Ca.pdos.ps
pause -1 "hit any key to continue\n"
```

Sr

```
set term postscript enhanced color 'Helvetica-Bold' 20
set output 'Sr.pdos.ps'
set autoscale
unset log
unset label
set xtic 10,1
set ytic auto
set xlabel "Energy (ev)"
set ylabel "Pdos"
set xr [0:10]
set yr [0:2]
```

```
set arrow from  5.1577,0.0 to  5.1577,2, 2 nohead ls 10 dt 2
plot  "atom_Sr_s.dat" using 1:2 title 'Sr s orbital' w l lw 3 lt 1 lc rgb "blue",\
     "atom_Sr_p.dat" using 1:2 title 'Sr p orbital' w l lw 3 lt 1 lc rgb "red",\
     "atom_Sr_tot.dat" using 1:2 title 'Sr total orbital' w l lw 3 lt 1 lc rgb "yellow",


set output
 ! ps2pdf Sr.pdos.ps
 ! rm Sr.pdos.ps
pause -1 "hit any key to continue\n"
```